

Silicon-Containing Polyphilic Bent-Core Molecules: The Importance of Nanosegregation for the Development of Chirality and Polar Order in Liquid Crystalline Phases Formed by Achiral Molecules

Christina Keith,[†] R. Amaranatha Reddy,[†] Anton Hauser,[‡] Ute Baumeister,[‡] and Carsten Tschierske^{*†}

Contribution from the Institute of Organic Chemistry, Martin-Luther University Halle-Wittenberg, Kurt-Mothes Strasse 2, D-06120 Halle, Germany, and Institute of Physical Chemistry, Martin-Luther University Halle-Wittenberg, Mühlporfte 1, D-06108 Halle, Germany

Received November 11, 2005; Revised Manuscript Received January 9, 2006; E-mail: carsten.tschierske@chemie.uni-halle.de

Abstract: Polyphilic molecules composed of a bent aromatic core, oligo(siloxane) units, and alkyl segments were synthesized, and the self-organization of these molecules was investigated. Most materials organize into polar smectic liquid crystalline phases. The switching process of these mesophases changes from antiferroelectric for the nonsilylated compounds via superparaelectric to surface-stabilized ferroelectric with increasing segregation of the silylated segments. It is proposed that the siloxane sublayers stabilize a polar synclitic ferroelectric (SmC_sP_F) structure, and the escape from a macroscopic polar order as well as steric effects leads to a deformation of the layers with formation of disordered microdomains, giving rise to optical isotropy. Another striking feature is the spontaneous formation of chiral domains with opposite handedness. For two compounds, a temperature-dependent inversion of the optical rotation of these domains was found, and this is associated with an increase of the tilt angle of the molecules from $<45^\circ$ to $>50^\circ$. This observation confirms the recently proposed concept of layer optical chirality (Hough, L. E.; Clark, N. A. *Phys. Rev. Lett.* **2005**, *95*, 107802), which is a new source of optical activity in supramolecular systems. With increasing length of the alkyl chains, segregation is lost and a transition from smectic to a columnar phase is found. In the columnar phase, the switching process is antiferroelectric and takes place by rotation of the molecules around the long axes, which reverses the layer chirality; that is, the racemic ground-state structure is switched into a homogeneous chiral structure upon application of an electric field.

Introduction

Supramolecular chemistry aims at developing complex systems from programmed molecules in a thermodynamically controlled self-assembly process.¹ Liquid crystals (LC) represent a special type of self-organized systems, which is fluid and has a well defined periodic nanoscale structure, giving rise to anisotropic physical properties. In addition, these materials can easily change their configuration under the influence of different external stimuli. This unique combination of long range order and mobility is also a basic requirement for the development of living matter and provides the foundation of numerous future technological applications. Early work on liquid crystalline (LC) materials gave quite simple (nematic, smectic, and columnar) phase structures,² which already find broad use, for example, as materials in displays of mobile communication and data processing devices. Future LC materials might, for example, provide new photonic materials,³ semiconducting organic

materials for electronic circuits and photovoltaics,⁴ switchable NLO materials, and sophisticated materials for optical switches and phase modulators.⁵ Hence, the fundamental understanding of the self-organization in such systems is of importance for future developments in science and technology. This requires the detailed understanding of the effects of molecular-structural parameters upon nanoscale morphologies and macroscopic properties of these systems. The introduction of molecular chirality⁶ and polyphilicity⁷ into LC materials has been used to provide novel, more complex self-organized LC structures,⁸ among them, cubic and other 3D phases,⁹ cylinder phases,^{8f,i,j,l,m,o,p,r}

[†] Institute of Organic Chemistry.

[‡] Institute of Physical Chemistry.

- (1) (a) Lehn, J.-M. *Proc. Natl. Acad. Sci. U.S.A.* **2002**, *99*, 4763–4768. (b) Lehn, J.-M. *Science* **2002**, *295*, 2400–2403.
(2) *Handbook of Liquid Crystals*; Demus, D., Goodby, J. W., Gray, G. W., Spiess, H.-W., Vill, V., Eds.; Wiley-VCH: Weinheim, Germany, 1998; Vols. 1–3.

- (3) (a) Coles, H. J.; Pivnenko, M. N. *Nature* **2005**, *436*, 997–1000. (b) Hwang, J.; Song, M. H.; Park, B.; Nishimura, S.; Toyooka, T.; Wu, J. W.; Takaniishi, Y.; Ishikawa, K.; Takezoe, H. *Nat. Mater.* **2005**, *4*, 382–387.
(4) (a) Simpson, C. D.; Wu, J.; Watson, M. D.; Müllen, K. *J. Mater. Chem.* **2004**, *14*, 494–504. (b) Schmidt-Mende, L.; Fechtenkötter, A.; Müllen, K.; Moons, E.; Friend, R. H.; MacKenzie, J. D. *Science* **2001**, *293*, 1119–1122.
(5) O'Callaghan, M. J.; Wand, M. D.; Walker, C. M.; Nakata, M. *Appl. Phys. Lett.* **2004**, *85*, 6344–6346.
(6) (a) Pansu, B. *Mod. Phys. Lett. B* **1999**, *13*, 769–782. (b) Kitzerow, H.-S.; Bahr, C. *Chirality in Liquid Crystals*; Springer: New York, 2001.
(7) (a) Tschierske, C. *J. Mater. Chem.* **1998**, *8*, 1485–1508. (b) Tschierske, C. *J. Mater. Chem.* **2001**, *11*, 2647–2671. (c) Tournilhac, F.; Blinov, L. M.; Simon, J.; Yablonsky, S. V. *Nature* **1992**, *359*, 621–623. (d) Ostrovskii, B. I. In *Structure and Bonding* **94**, *Liquid Crystals I*; Mingos, D. M. P., Ed.; Springer: Berlin, 1999; pp 200–240.

quasi liquid crystalline phases,¹⁰ and LC phases showing ferroelectric (FE) and antiferroelectric (AF) properties.^{6b}

Reduction of the symmetry of rigid segments is an additional way to increase the complexity of LC superstructures. This was shown for molecules with a bent aromatic core structure (banana-shaped LC), which can give rise to macroscopic polar order in fluid systems.¹¹ Polar order results from the packing of the bent-core molecules in layers where the bent structure restricts their rotation around the long axis, leading to a spontaneous polarization (P) parallel to the layer planes.¹² In adjacent layers, both tilt direction and polar direction can be either identical or opposite, leading to, in total, four different structures, as shown in Figure 1.¹³ Two of them are macroscopically polar (SmC_sP_F and SmC_aP_F); the others are macroscopically nonpolar (SmC_aP_A and SmC_sP_A). Usually, the AF states (SmC_aP_A and SmC_sP_A) are stable and can be switched into the corresponding FE states (SmC_sP_F and SmC_aP_F , respectively) under the influence of an external electric field. Upon switching off the field, the polar FE states usually relax back to the nonpolar AF states. This switching process has three stable states and therefore represents an AF switching process.

We have recently enhanced the complexity of bent-core molecules by introduction of an additional incompatible unit, leading to a new class of liquid crystals composed of three incompatible units: a bent rigid aromatic core, two flexible alkyl chains, and a highly flexible and bulky oligosiloxane end group at one terminus.¹⁴ These *polyphilic bent-core molecules* combine two fundamental concepts of LC design, the concept of polyphilicity⁷ and the concept of bent-core molecules. The molecules are abbreviated as $\text{Si}_x\text{-mBn}$, where x gives the number

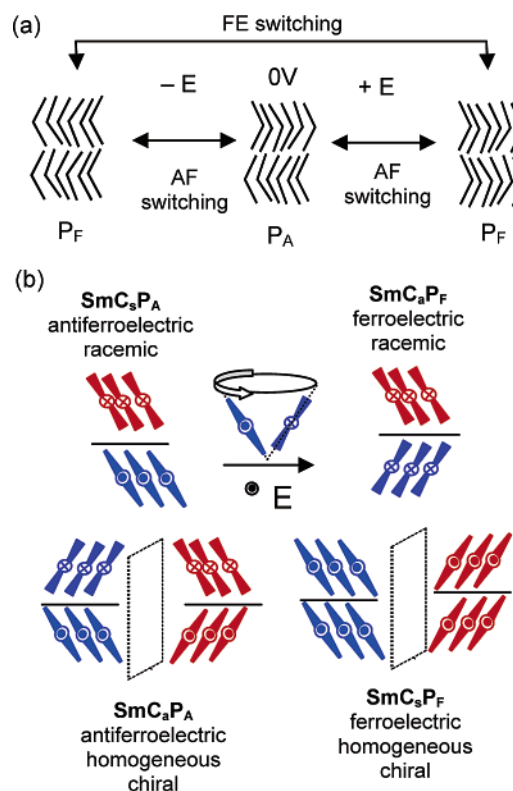
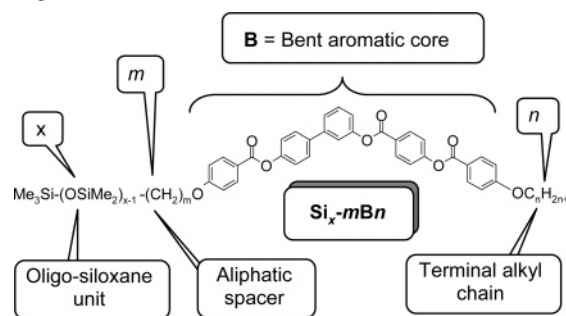


Figure 1. (a) The switching of bent-core molecules (side views) and (b) the four possible arrangements in tilted polar smectic phases. The subscripts 's' and 'a' indicate the correlation of the tilt direction in adjacent layers: s = synclinal means an identical tilt direction; a = anticlinal indicates an opposite tilt direction. Subscripts 'A' and 'F' indicate the correlation of the polar direction in adjacent layers. P_A is indicative of an antipolar structure (polar direction alternates); this structure is macroscopically nonpolar and usually assigned as antiferroelectric. P_F stands for a synpolar structure (polar direction is identical); this structure is macroscopically polar and usually assigned as ferroelectric (and therefore abbreviated as P_F). The color indicates the chirality of the layers (*superstructural chirality*; for details, see Figure S1 in Supporting Information). The SmC_aP_A and SmC_sP_F structures are homogeneous chiral (identical chirality sense in the layers), and the SmC_sP_A and SmC_aP_F structures are macroscopic racemic (alternating chirality sense in the layers). Switching usually takes place on a cone (shown in the middle). It reverses polar direction and tilt direction and retains the layer chirality.

Scheme 1. Structure and Assignment of the Compounds under Investigation



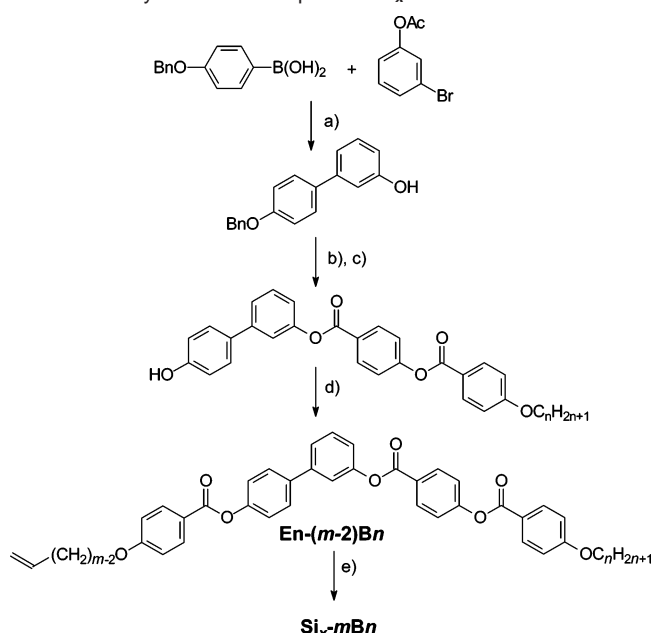
of Si atoms in the siloxane units, m the length of the spacer unit between siloxanes and bent cores; **B** stands for the bent-core unit, and n is the number of C atoms in the terminal alkyl chain (see Scheme 1). Three of such compounds ($\text{Si}_x\text{-11B12}$ with $x = 2, 3, i3$) have been reported in a previous communication.¹⁴ It turned out that the siloxane units have a large impact on the properties of the mesophases of these molecules. It leads to a change of the switching behavior from AF to an apparently

- (8) (a) Tschierske, C. *Ann. Rep. Prog. Chem., Ser. C* **2001**, 97, 191–267. (b) Goodby, J. W.; Mehl, G. H.; Saez, I. M.; Tuffin, R. P.; Mackenzie, G.; Auzély-Velty, R.; Benvegnu, T.; Plusquellec, D. *Chem. Commun.* **1998**, 2057–2070. (c) Lee, M.; Cho, B.-K.; Zin, W.-C. *Chem. Rev.* **2001**, 101, 3869–3892. (d) Kato, T. *Science* **2002**, 295, 2414–2418. (e) Barberá, J.; Donnio, B.; Giménez, R.; Guillon, D.; Marcos, M.; Omenat, A.; Serrano, J. L. *J. Mater. Chem.* **2001**, 11, 2808–2813. (f) Köbel, M.; Beyersdorff, T.; Cheng, X. H.; Kain, J.; Diele, S. *J. Am. Chem. Soc.* **2001**, 123, 6809–6818. (g) Tschierske, C. *Curr. Opin. Colloid Interface Sci.* **2002**, 7, 69–80. (h) Gehringer, L.; Bourgogne, C.; Guillon, D.; Donnio, B. *J. Am. Chem. Soc.* **2004**, 126, 3856–3867. (i) Cheng, X. H.; Prehm, M.; Das, M. K.; Kain, J.; Baumeister, U.; Diele, S.; Leine, D.; Blume, A.; Tschierske, C. *J. Am. Chem. Soc.* **2003**, 125, 10977–10996. (j) Chen, B.; Zeng, X.; Baumeister, U.; Diele, S.; Ungar, G.; Tschierske, C. *Angew. Chem., Int. Ed.* **2004**, 43, 4621–4625. (k) Oh, N.-K.; Zin, W.-C.; Im, J.-H.; Ryu, J.-H.; Lee, M. *Chem. Commun.* **2004**, 1092–1093. (l) Cheng, X.; Das, M. K.; Baumeister, U.; Diele, S.; Tschierske, C. *J. Am. Chem. Soc.* **2004**, 126, 12930–12940. (m) Chen, B.; Baumeister, U.; Das, M. K.; Zeng, X.; Ungar, G.; Tschierske, C. *J. Am. Chem. Soc.* **2004**, 126, 8608–8609. (n) Saez, I. M.; Goodby, J. W. *J. Mater. Chem.* **2005**, 15, 26–40. (o) Cook, A. G.; Baumeister, U.; Tschierske, C. *J. Mater. Chem.* **2005**, 15, 1708–1721. (p) Chen, B.; Zeng, X. B.; Baumeister, U.; Ungar, G.; Tschierske, C. *Science* **2005**, 307, 96–99. (q) Schaz, A.; Lattermann, G. *Liq. Cryst.* **2005**, 32, 407–415. (r) Chen, B.; Baumeister, U.; Pelzl, G.; Das, M. K.; Zeng, B.; Ungar, G.; Tschierske, C. *J. Am. Chem. Soc.* **2005**, 127, 16578–16591. (s) Ungar, G.; Zeng, X. *Soft Matter* **2005**, 1, 95–106. (9) (a) Diele, S. *Curr. Opin. Colloid Interface Sci.* **2002**, 7, 333–342. (b) Borisch, K.; Diele, S.; Göring, P.; Kresse, H.; Tschierske, C. *J. Mater. Chem.* **1998**, 8, 529–543. (c) Ungar, G.; Liu, Y.; Zeng, X.; Percec, V.; Cho, W.-D. *Science* **2003**, 299, 1208–1211. (d) Percec, V.; Mitchell, C. M.; Cho, W.-D.; Uchida, S.; Glodde, M.; Ungar, G.; Zeng, X.; Liu, Y.; Balagurusamy, V. S. K.; Heiney, P. A. *J. Am. Chem. Soc.* **2004**, 126, 6078–6094. (10) Zeng, X.; Ungar, G.; Liu, Y.; Percec, V.; Dulcey, A. E.; Hobbs, J. K. *Nature* **2004**, 428, 157–160. (11) Niori, T.; Sekine, T.; Watanabe, J.; Furukawa, T.; Takezoe, H. *J. Mater. Chem.* **1996**, 6, 1231–1233. (12) Reviews: (a) Pelzl, G.; Diele, S.; Weissflog, W. *Adv. Mater.* **1999**, 11, 707–724. (b) Tschierske, C.; Dantlgraber, G. *Pramana* **2003**, 61, 455–481. (c) Amaranatha Reddy, R.; Tschierske, C. *J. Mater. Chem.* **2005**, DOI 10.1039/b504400f. (13) (a) Link, D. R.; Natale, G.; Shao, R.; MacLennan, J. E.; Clark, N. A.; Körblöva, E.; Walba, D. M. *Science* **1997**, 278, 1924–1927. (b) Walba, D. M. *Topics in Stereochemistry (Materials-Chirality)*; Green, M. M., Nolte, R. J. M., Meijer, E. W., Eds.; Wiley: New York, 2003; Vol. 42, p 475.

ferroelectric type, and also the optical appearance of the mesophase is completely changed. The highly birefringent textures usually observed for smectic phases are replaced by optically isotropic phases composed of chiral domains with opposite handedness. In the meanwhile, these “dark conglomerate phases” were observed for several other bent-core molecules with FE or AF switching smectic phases.^{15–18} Recently, a related phenomenon was also observed in a cubic mesophase.¹⁹ However, though the subject of intensive discussions, the origin of optical isotropy, chirality, and ferroelectricity remained unclear.

To clarify the situation, we performed a systematic study, concerning the influence of the molecular structure of these oligosiloxane-derived polyphilic bent-core LCs upon their self-organization in LC phases, which is reported herein. The most important result is that two of these compounds show a temperature-dependent inversion of the optical rotation. This is the first report on a temperature-induced inversion of chirality in a supramolecular system formed by achiral molecules. This observation, together with the recently proposed concept of layer optical chirality,²⁰ allows now for the first time one to assign the phase structure of the dark conglomerate phases of the investigated compounds as synclinic tilted and ferroelectric ($\text{SmC}_\text{sP}_\text{F}$). This leads to a fundamental understanding of the self-organization in these systems and the switching behavior of these mesophases. The $\text{SmC}_\text{sP}_\text{F}$ organization is stabilized as the segregation of oligosiloxane segments is increased, and this is a function of the size of the oligosiloxane units, but also alkyl chain length and spacer length are important. A transition from

Scheme 2. Synthesis of Compounds $\text{Si}_x\text{-mBn}^a$



^a Reagents and conditions: (a) cat. $[\text{Pd}(\text{PPh}_3)_4]$, NaHCO_3 , H_2O , glyme, reflux, 8 h;²³ (b) 4-(4-*n*-alkoxybenzoyloxy)benzoic acid,²⁶ DCC, DMAP, CH_2Cl_2 , 20 °C, 24 h;²⁴ (c) H_2 , Pd/C, THF, 40 °C, 16 h; (d) 4-(ω -alkenyloxy)benzoic acid,²⁵ DCC, DMAP, CH_2Cl_2 , 20 °C, 24 h;²⁴ (e) EtMe_2SiH ($x = 1$) or $\text{Me}_3\text{Si}(\text{OMe}_2\text{Si})_{x-1}\text{H}$ ($x = 2, 3$), Karstedt's catalyst, toluene, 20 °C, 24 h.^{14,22}

AF via superparaelectric to surface-stabilized FE switching is found with increasing segregation. In addition, with increasing length of the alkyl chains, a transition from smectic phases via wavy deformed layers to a columnar phase is found, which is mainly due to steric reasons. In contrast to the smectic phases, in the columnar phase, the switching process is antiferroelectric and takes place by rotation of the molecules around the long axes, which reverses the superstructural chirality; that is, the racemic nonpolar ground-state structure is switched into a homogeneous chiral polar structure upon application of an electric field. These results provide a lesson in principles of self-assembly in polar ordered soft matter and offer fundamental clues for future design of new bent-core mesogens with specific properties, namely, superstructural chirality and polar order, in a predictable way.

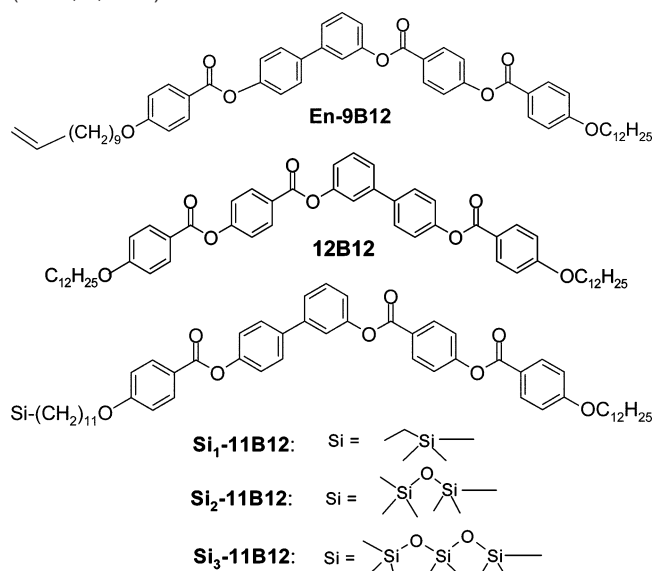
Results and Discussion

1. Synthesis. The synthesis of the compounds is shortly outlined in Scheme 2. Accordingly, compounds **En-(*m*-2)Bn** with a terminal double bond were synthesized first,²¹ and in the final step, the silicon-containing units were attached by hydrosilylation reaction, yielding the silylated derivatives **Si_x-mBn**.^{14,22} Isolation and purification was achieved by repeated chromatography and crystallization. The experimental procedures and analytical data are described in the Supporting Information. The characterization of the mesophases was done

- (14) Preliminary communication: Dantlgraber, G.; Eremin, A.; Diele, S.; Hauser, A.; Kresse, H.; Pelzl, G.; Tschierske, C. *Angew. Chem., Int. Ed.* **2002**, *41*, 2408–2412.
- (15) (a) Thisayukta, J.; Nakayama, Y.; Kawauchi, S.; Takezoe, H.; Watanabe, J. *J. Am. Chem. Soc.* **2000**, *122*, 7441–7448. (b) Thisayukta, J.; Kamee, H.; Kawauchi, S.; Watanabe, J. *Mol. Cryst. Liq. Cryst.* **2000**, *346*, 63–75. (c) Shreenivasa Murthy, H. N.; Sadashiva, B. K. *Liq. Cryst.* **2002**, *29*, 1223–1234. (d) Ortega, J.; Folcia, C. L.; Etxebarria, J.; Gimeno, N.; Ros, M. B. *Phys. Rev. E* **2003**, *68*, 011707. (e) Weissflog, W.; Schröder, M. W.; Diele, S.; Pelzl, G. *Adv. Mater.* **2003**, *15*, 630–633. (f) Jakli, A.; Huang, Y.-M.; Fodor-Csorba, K.; Vajda, A.; Galli, G.; Diele, S.; Pelzl, G. *Adv. Mater.* **2003**, *15*, 1606–1610. (g) Schröder, M. W.; Diele, S.; Pelzl, G.; Dunemann, U.; Kresse, H.; Weissflog, W. *J. Mater. Chem.* **2003**, *13*, 1877–1882. (h) Schröder, M. W.; Pelzl, G.; Dunemann, U.; Weissflog, W. *Liq. Cryst.* **2004**, *31*, 633–637. (i) Weissflog, W.; Sokolowski, S.; Dehne, H.; Das, B.; Grande, S.; Schröder, M. W.; Eremin, A.; Diele, S.; Pelzl, G.; Kresse, H. *Liq. Cryst.* **2004**, *31*, 923–933.
- (16) Field-induced $\text{SmCP}^{[*]}$ phases: (a) Heppke, G.; Parghi, D. D.; Sawade, H. *Liq. Cryst.* **2000**, *27*, 313–320. (b) Etxebarria, J.; Folcia, C. L.; Ortega, J.; Ros, M. B. *Phys. Rev. E* **2003**, *67*, 042702.
- (17) Bent-core dimers and oligomers and polymers based on oligosiloxane and carbosilane units: (a) Dantlgraber, G.; Diele, S.; Tschierske, C. *Chem. Commun.* **2002**, 2768–2769. (b) Dantlgraber, G.; Baumeister, U.; Diele, S.; Kresse, H.; Lüthmann, B.; Lang, H.; Tschierske, C. *J. Am. Chem. Soc.* **2002**, *124*, 14852–14853. (c) Keith, C.; Amaranatha Reddy, R.; Tschierske, C. *Chem. Commun.* **2005**, 871–873. (d) Keith, C.; Amaranatha Reddy, R.; Hahn, H.; Lang, H.; Tschierske, C. *Chem. Commun.* **2004**, 1898–1899. (e) Hahn, H.; Lang, H.; Tschierske, C. *Chem. Commun.* **2004**, 1898–1899. (f) Rauch, S.; Bault, P.; Sawade, H.; Heppke, G.; Nair, G. G.; Jakli, A. *Phys. Rev. E* **2002**, *66*, 021706. (g) Kumazawa, K.; Nakata, M.; Araoka, F.; Takanishi, Y.; Ishikawa, K.; Watanabe, J.; Takezoe, H. *J. Mater. Chem.* **2004**, *14*, 157–164. (h) Amaranatha Reddy, R.; Raghunathan, V. A.; Sadashiva, B. K. *Chem. Mater.* **2005**, *17*, 274–283. (i) Nadasi, H.; Weissflog, W.; Eremin, A.; Pelzl, G.; Diele, S.; Das, S.; Grande, S. *J. Mater. Chem.* **2002**, *12*, 1316–1324. (j) Bedel, J. P.; Rouillon, J. C.; Marcerou, J. P.; Nguyen, H. T.; Achard, M. F. *J. Mater. Chem.* **2002**, *12*, 2214–2220. (d) Amaranatha Reddy, R.; Sadashiva, B. K. *J. Mater. Chem.* **2002**, *12*, 2627–2642. (e) Amaranatha Reddy, R.; Sadashiva, B. K. *Liq. Cryst.* **2003**, *30*, 1031–1050. (f) Rauch, S.; Bault, P.; Sawade, H.; Heppke, G.; Nair, G. G.; Jakli, A. *Phys. Rev. E* **2002**, *66*, 021706. (g) Kumazawa, K.; Nakata, M.; Araoka, F.; Takanishi, Y.; Ishikawa, K.; Watanabe, J.; Takezoe, H. *J. Mater. Chem.* **2004**, *14*, 157–164. (h) Amaranatha Reddy, R.; Raghunathan, V. A.; Sadashiva, B. K. *Chem. Mater.* **2005**, *17*, 274–283. (i) Nadasi, H.; Weissflog, W.; Eremin, A.; Pelzl, G.; Diele, S.; Das, S.; Grande, S. *J. Mater. Chem.* **2002**, *12*, 1316–1324. (j) Bedel, J. P.; Rouillon, J. C.; Marcerou, J. P.; Nguyen, H. T.; Achard, M. F. *Phys. Rev. E* **2004**, *69*, 061702. (k) Takezoe, H.; et al. *J. Am. Chem. Soc.* **2005**, *127*, 11085–11091.
- (19) Kajitani, T.; Kohmoto, S.; Yamamoto, M.; Kishikawa, K. *Chem. Mater.* **2005**, *17*, 3812–3819.
- (20) Hough, L. E.; Clark, N. A. *Phys. Rev. Lett.* **2005**, *95*, 107802.

- (21) Transition temperatures and transition enthalpies of compounds **En-(*m*-2)Bn** are collated in Tables S2 and S3 of the Supporting Information. In the series of the olefins **En-9Bn** with increasing chain length, nonswitching rectangular columnar phases ($n = 4–8$; B_1 phases, see Figure S4) are replaced by AF switching polar smectic C phases ($n = 10–22$), characterized by a single-layer structure without in-plane order and birefringent textures (SmCP_A phases = B_2 -type phases). This B_1 – B_2 sequence is usually observed in the homologous series of bent-core molecules upon elongation of alkyl chains; see ref 26.
- (22) Mehl, G. H.; Goodby, J. W. *Chem. Ber.* **1996**, *129*, 521–525.

Table 1. Mesophases, Phase Transition Temperatures, and *d* Values of the Smectic Phases of the Bent-Core Molecules **12B12** and **En-9B12**¹⁴ and the Silylated Derivatives **Si_x-11B12** (*x* = 1, 2,¹⁴ 3¹⁴)



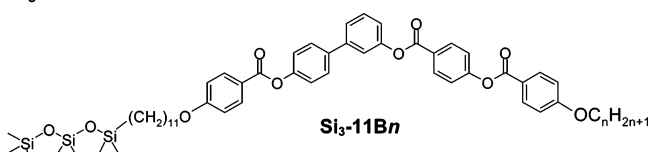
compound	<i>T</i> /°C ^a	<i>d</i> /nm (<i>T</i> /°C)	<i>L</i> /nm ^b
En-9B12 ^c	Cr 108 (SmCP _A 98) Iso	n.d.	
12B12	Cr 88 SmCP _A 111 Iso	3.7 (90)	5.2
Si₁-11B12	Cr 100 SmC _s P _F ^[*/*] 114 Iso	3.9 (105)	5.4
Si₂-11B12 ^c	Cr 77 SmC _s P _F ^[*/*] 118 Iso	4.2 (95)	5.6
Si₃-11B12 ^c	Cr 70 SmC _s P _F ^[*/*] 115 Iso	4.4 (95)	5.8
Si₁₃-11B12 ^{c,d}	Cr 63 SmC _s P _F ^[*/*] 116 Iso	n.d.	

^a Abbreviations: Cr = crystalline solid state; Iso = isotropic liquid state; SmCP_A = tilted polar smectic phase with antipolar structure; SmC_sP_F^[*/*] = distorted synclinal tilted polar smectic phase with synpolar order and chiral domains of opposite handedness in the ground state; [*/*] indicates that macroscopic chiral domains coexist with a birefringent texture; g = glass transition; n.d. = not determined. ^b *L* = molecular length assuming an overall V-shaped conformation with a bending angle of 120°, *all-trans* conformation of the alkyl chains and most stretched conformation of the Si-containing units. ^c See ref 14. ^d Branched oligosiloxane unit (2-substituted 1,1,1,2,3,3,3-heptamethyltrisiloxane).

by polarizing microscopy, differential scanning calorimetry (DSC), X-ray scattering, and investigation of the switching behavior by electrooptical methods.

2. Mesomorphic Properties. 2.1. Size of the Silicon-Containing Unit: Transition from Conventional SmCP_A Phases to Dark Conglomerate Phases. The phase transition temperatures of the synthesized compounds **Si_x-mBn** are collated in Tables 1–3. In Table 1, the influence of the size of the Si-containing unit upon the liquid crystalline properties is shown for the dodecyl-substituted compounds **Si_x-11B12** (*x* = 1–3), and these compounds are compared with the olefinic precursor **En-9B12**¹⁴ and the alkyl-substituted compound **12B12**. The nonsilylated and terminally unsaturated compound **En-9B12** has a monotropic (metastable) birefringent AF switching SmCP_A phase (B₂-type phase) as typical for numerous other bent-core molecules and also found for the dialkyl-substituted compound **12B12** without C=C double bond (see Figures S2 and S3). Hydrosilylation²² of **En-9B12**¹⁴ leads to the silyl-substituted materials **Si_x-11B12** (*x* = 1–3), which show enantiotropic (thermodynamically stable) mesophases with enhanced mesophase stability compared to **12B12** and **En-9B12**, despite that the Si-containing units are more bulky than linear

Table 2. Mesophases and Phase Transitions of Compounds **Si₃-11Bn**^a



<i>n</i>	<i>T</i> /°C Δ <i>H</i> /kJ mol ^{−1b}	<i>d</i> , <i>a</i> , <i>b</i> /nm, γ/°	<i>L</i> /nm
1	Cr 130 Iso 38.7		
4	Cr 93 SmC _s P _F ^[*/*] 10.9	113 Iso 17.1	4.4
6	Cr 100 SmC _s P _F ^[*/*] 31.6	118 Iso 20.9	5.2
8	Cr 94 SmC _s P _F ^[*/*] 20.3	117 Iso 18.3	5.4
10	Cr 61 SmC _s P _F ^[*/*] 12.5	117 Iso 22.3	5.6
11	Cr 63 SmC _s P _F ^[*/*] 30.2	113 Iso 22.3	5.7
12	Cr 70 SmC _s P _F ^[*/*] 29.3	115 Iso 24.3	5.8
14	Cr 61 (SmX ^l 60) 22.6	SmC _s P _F ^[*/*] 113 Iso 11.4 20.4	4.5 3.7 ^c
16	Cr 66 SmC _s P _F ^[*/*] 23.9	111 Iso 22.9	4.5
18	Cr 87 USmC _s P _F [′] 23.9	96 USmC _s P _F 109 Iso 1.8 16.3	4.4
20	Cr 83 USmC _s P _F [′] 22.5	96 Col _{ob} P _A 100 Iso 17.3	4.4 ^d 4.5, 2.2, 103°
22	Cr 88 Col _{ob} P _A 28.8	98 Iso 13.1	4.9, 2.2, 100°

^a Abbreviations: USmC_sP_F, USmC_sP_F[′] = undulated (wavy deformed) polar smectic phases with synclinal and synpolar correlation between adjacent layers (see Figure 9b); Col_{ob}P_A = AF switching oblique columnar phase (see Figure 9c); SmX^l = nonswitchable smectic phase with additional in-plane order; values in parentheses indicate monotropic (metastable) mesophases; for other abbreviations, see Table 1. ^b Determined by DSC, first heating scan, 10 K min^{−1}. ^c Refers to the SmX^l phase. ^d Refers to the USmC_sP_F phase

alkyl chains and therefore were expected to reduce the stability of LC phases.

However, the mesophases of the silylated compounds are quite distinct from those formed by related nonsilylated molecules.²⁶ These mesophases appear as fractal nuclei which coalesce to a grainy unspecific texture which is completely dark (optically isotropic) between crossed polarizers, showing only very small irregularly distributed bright spots in some cases. A remarkable feature of the mesophases of compounds **Si_x-11B12** and **Si₃-11Bn** (*n* = 4–16) is that, in these mesophases, domains of opposite handedness can be distinguished, as shown for the mesophase of **Si₃-11B14**, as an example, in Figure 2a,b. Upon rotating the analyzer by a small angle (5–10°), dark and bright domains become visible. If the analyzer is rotated in the opposite direction, the brightness of the domains is reversed. The light transmission does not change if the sample is rotated. This indicates a conglomerate of macroscopic chiral domains with opposite chirality sense. These optically isotropic mesophases composed of a conglomerate of chiral domains are designated

- (23) (a) Miyaura, N.; Suzuki, A. *Chem. Rev.* **1995**, 95, 2457–2483. (b) Hird, M.; Gray, G. W.; Toyne, K. J. *Mol. Cryst. Liq. Cryst.* **1991**, 206, 187–204.
 (24) Tschierske, C.; Zschke, H. J. *Prakt. Chem.* **1989**, 331, 365–366.
 (25) Adams, N. W.; Bradshaw, J. S.; Bayona, J. M.; Markides, K. E.; Lee, M. L. *Mol. Cryst. Liq. Cryst.* **1987**, 147, 43–60.
 (26) Shen, D.; Pegenau, A.; Diele, S.; Wirth, I.; Tschierske, C. *J. Am. Chem. Soc.* **2000**, 122, 1593–1601.

Table 3. Mesophases and Phase Transitions of Compounds **Si₃-mB12**^a

compound	<i>m</i>	<i>T</i> /°C ΔH /kJ mol ⁻¹		<i>d</i> /nm	<i>L</i> /nm
Si₃-5B12	5	Cr 105 (SmC _s P _F ^[*/*] 83) Iso 53.2			
Si₃-6B12	6	Cr 86 SmC _s P _F ^[*/*] 18.1	93 Iso 14.8	4.8 (85)	5.3
Si₃-7B12	7	Cr 75 SmC _s P _F ^[*/*] 21.3	104 Iso 20.6	3.8 (90)	5.4
Si₃-8B12	8	Cr 71 SmC _s P _F ^[*/*] 21.8	102 Iso 16.3	4.0 (90)	5.5
Si₃-9B12	9	Cr ₁ 58 Cr ₂ 28.8	68 (SmX ^[*] 61) SmC _s P _F ^[*] 11.9	108 Iso 21.1	5.6
Si₃-10B12	10	Cr 63 SmC _s P _F ^[*] 39.2	115 Iso 22.3	4.4 (97)	5.7
Si₃-11B12	11	Cr 70 SmC _s P _F ^[*] 115 Iso		4.4 (95)	5.8

^a Abbreviations and conditions as in Tables 1 and 2.

as “dark conglomerate phases”, and this type of supramolecular chirality, which is *not* based on a molecular configurational chirality, is assigned with the symbol “[*]”. For all compounds with a heptamethyltrisiloxane unit (**Si₃-11B n** with $n = 4–16$ and **Si₃-11B12**), this dark conglomerate texture is found exclusively. However, for compounds **Si₁-11B12** and **Si₂-11B12** with shorter Si-containing units, sometimes also regions with a birefringent schlieren texture can coexist with the dark conglomerate texture (assigned with [*/*]).

X-ray investigations indicate simple layer structures without in-plane order for the mesophases of all compounds **Si_x-11B12** ($x = 1–3$). The layer thickness is always significantly smaller than the molecular length, which is in line with a strongly tilted arrangement of the molecules within a monolayer structure with estimated tilt angles of about 35–45° with respect to the layer normal (SmCP phases).

In addition, there is an important change in the profile of the diffuse wide-angle scattering. For compound **Si₃-11B12** with a large oligosiloxane unit, this scattering has a very asymmetric profile in which two maxima can be separated, one maximum at 0.47 nm corresponding to the mean distance between the fluid alkyl chains and between the aromatic cores and the second one with a maximum at about 0.7 nm corresponding to the mean distance between the disordered siloxane units (see for example curve “a” in Figure 4, which actually shows the wide-angle scattering of the higher homologue **Si₃-11B14**). This is an indication of the fluid nanosegregated organization in the smectic mesophase of this compound; that is, the siloxane units build up their own sublayers, leading to the triple layer structure, as shown in Figure 3a. The presence of different mean distances between hydrocarbon units (cross sectional area = 0.21 nm²) and between siloxane units (cross sectional area = 0.38 nm²) can be realized by adopting an antiparallel packing of adjacent molecules, leading to a monolayer structure instead of the expected bilayer structure.

The diffuse wide-angle reflection at $D = 0.7$ nm is missing for compounds **Si₁-11B12** and **Si₂-11B12** with smaller silicon-containing segments, which means that for these compounds the alkyl chains and the Si-containing units are not segregated (there are only two instead of three sublayers; see Figure 3b).

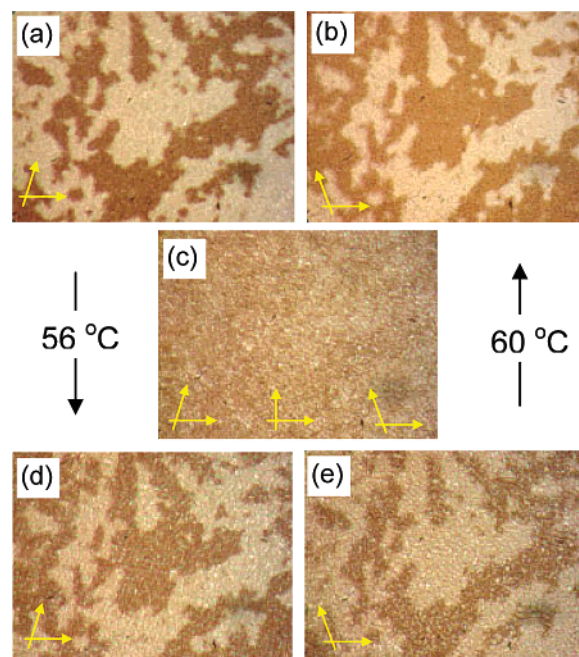


Figure 2. Chiral domains observed for compound **Si₃-11B14** (a), (b) in the SmC_sP_F^[*] phase at 65 °C between slightly uncrossed polarizers (arrows indicate the positions of the polarizers); (c) same region between crossed polarizers; (d, e) SmX^[*] phase at 55 °C between slightly uncrossed polarizers; from (a) to (b) and from (d) to (e), the direction of the polarizers is changed, from (a) via (c) to (d), the sample is cooled, from (e) via (c) to (b), it is heated. Texture (c) is actually observed in the SmC_sP_F^[*] phase at 65 °C under crossed polarizers, but the same appearance can be found at the transition from (a) to (d) and (e) to (b) depending on the temperature.

This correlates with the observed differences in the textural features between these compounds.

2.2. Effect of the Length of the Terminal Alkyl Chains: Transition from Smectic to Columnar Phases. As shown in Table 2, with increasing length of the terminal chain of compounds **Si₃-11B n** , a series of different mesophases is found, which is discussed in the following sections.

2.2.1. The Fluid Dark Conglomerate Smectic Phases of Compounds Si₃-11B4 to Si₃-11B16. All compounds **Si₃-11B n** with $n = 4–16$ show the same textural features as **Si₃-11B12**

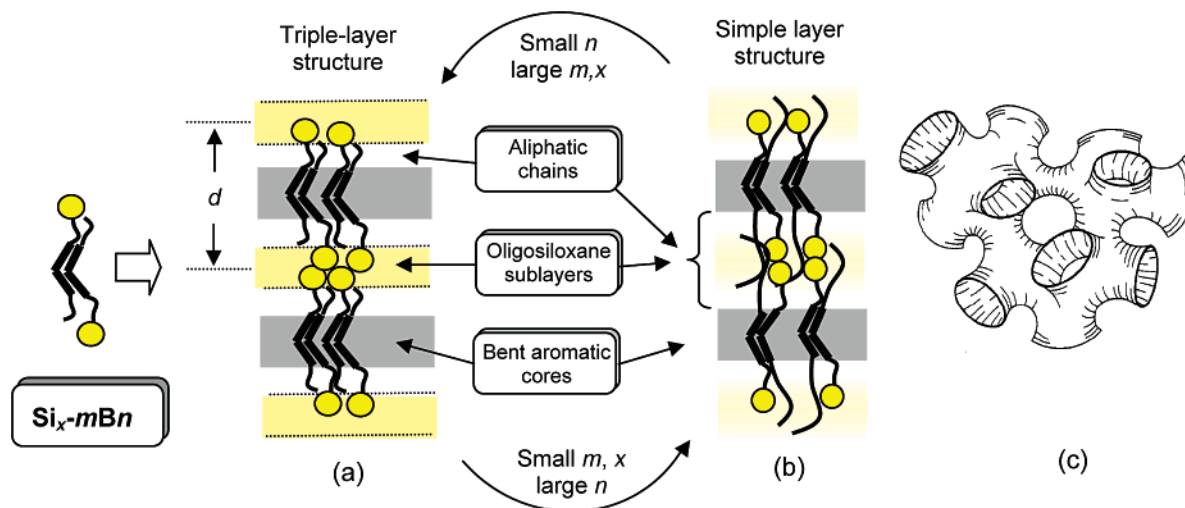


Figure 3. Models of the organization of the siloxane-substituted bent-core molecules (a) in the triply segregated smectic phases, and (b) in the simple smectic phases where aliphatic chains and oligo(dimethylsiloxane) units are not segregated; (c) shows the a model of a sponge phase (from ref 28a), where a random web of the aromatic layers divides the fluid regions (segregated oligosiloxane sublayers are not shown).

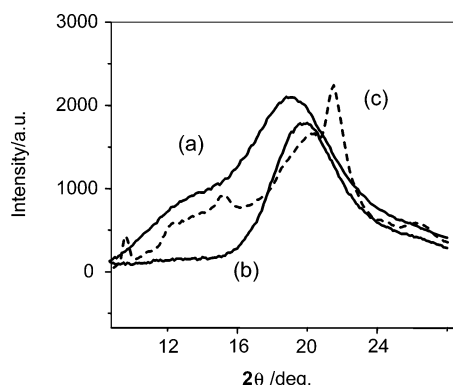


Figure 4. Wide-angle region of selected X-ray diffraction pattern: (a) two diffuse maxima in the $\text{SmC}_s\text{P}_F^{[*]}$ phase of compound **Si₃-11B14** at 100 °C indicate a nanosegregated structure with discrete oligosiloxane sublayers; (b) one diffuse maximum in the USmC_sP_F phase of compound **Si₃-11B18** at 92 °C indicates the absence of separate oligosiloxane sublayers; (c) several reflections in the $\text{SmX}^{[*]}$ phase of compound **Si₃-11B14** at 50 °C indicate an additional in-plane order.

(dark conglomerates). X-ray investigations confirm smectic phases without in-plane order (see Table S1 in the Supporting Information). Remarkably, there is no change of the layer distance on increasing the length of the alkyl chain. Compounds **Si₃-11B4** ($d = 4.4$ nm) and **Si₃-11B16** ($d = 4.5$ nm) have practically the same d value, though the difference of the molecular length is 12 CH_2 groups (see Table 2 and Figure 5)! This unique behavior is in line with the suggested triple layer model shown in Figure 3a. This means that the layer thickness is exclusively determined by the combined lengths of the spacer unit, bent-core, and siloxane unit. The alkyl end chains have to be accommodated within the sublayers provided by the spacer units. For molecules with extremely long chains, however (compounds **Si₃-11Bn** with $n = 18$ –22), this is not possible and segregation of alkyl chains and siloxane units is lost. This is seen in the profile of the diffuse wide-angle scattering in the X-ray diffraction pattern. For the smectic phases of all compounds **Si₃-11Bn** with $n = 4$ –14, there is a shoulder at $D = 0.7$ nm, corresponding to the mean distance between the siloxane units (see Figure 4, curve a). This shoulder is very weak for compound **Si₃-11B16**, and it is completely absent for the

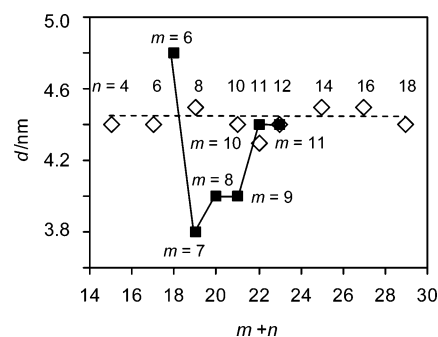


Figure 5. Dependence of the d values of the smectic phases of compounds **Si₃-mBn** on the number of C atoms m in the spacer unit (compounds **Si₃-mB12**, $n = 12$, filled squares and solid line) and on the number of C atoms n in the terminal alkyl chains (compounds **Si₃-11Bn**, $m = 11$, open squares and dotted line).

mesophases of compounds **Si₃-11Bn** with $n = 18$ –22 (see Figure 4, curve b, which shows the wide-angle profile of the wavy deformed smectic phase (USmC_sP_F) of compound **Si₃-11B18**).

The optical isotropy and the spontaneous formation of domains with opposite chirality sense are quite unusual features of the ground-state structures of the smectic mesophases of compounds **Si₃-11Bn** with $n = 4$ –16. As suggested by Jakli et al.,^{15f} an optical isotropic tilted smectic phase can be explained if the organization would be SmC_aP_A and if the bending angle α and tilt angle θ are related to each other according to $\alpha = 2 \tan^{-1}(1/\cos \theta)$. However, this uniform ratio is unlikely to occur for a whole series of compounds. In addition, as will be shown in section 3, the actual mesophase structure is synclinic and synpolar in most cases. Another remarkable feature of these mesophases is the disordered structure of the layers which can even be observed under the polarizing microscope in some cases (grainy appearance). Also, the diffraction peaks are not resolution limited, indicating a limited size of the smectic domains. AFM (see Figure 6) and electron microscopy with freeze fracture samples²⁷ confirm a strongly distorted structure of the layers (the layers are strongly folded), similar to lyotropic sponge

(27) Clark, N. A.; et al. Poster Presented at the 9th International Liquid Crystal Conference, Ljubljana, July 4–9, 2004, Book of Abstracts, SYN-P026.

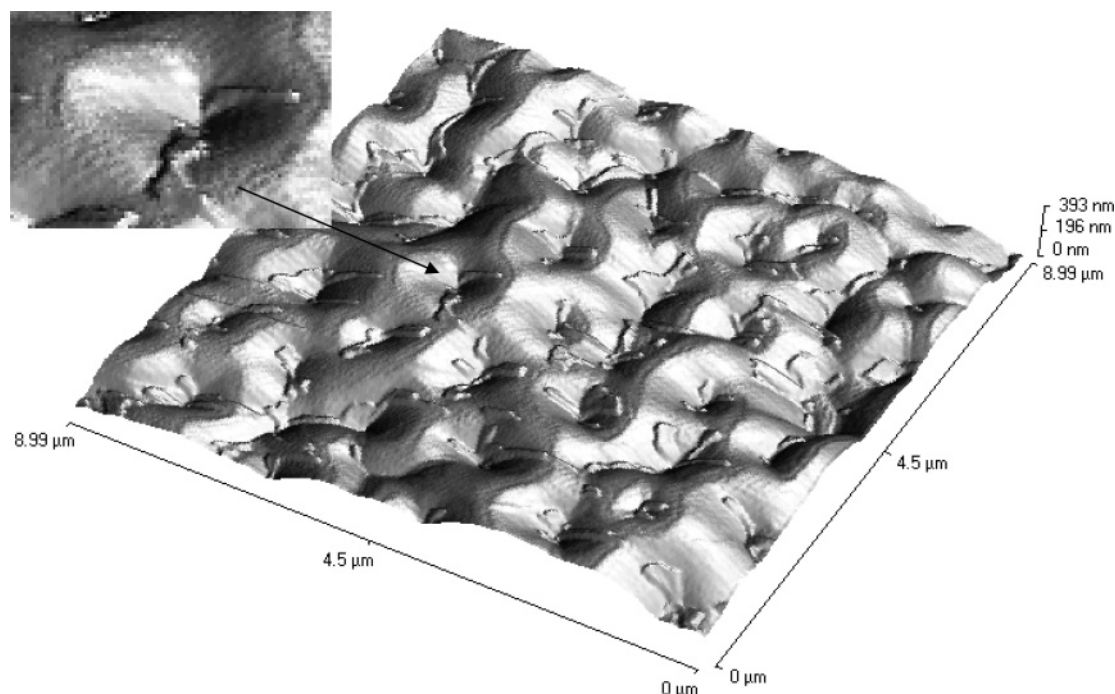


Figure 6. AFM image of the surface of a glassy solidified sample of the $\text{SmC}_s\text{P}_F^{[*]}$ phase of compound **Si₃-11B12** at 20 °C, showing a very rough surface structure. Beside the long-scale modulation, there is an additional fine grainy structure with a length scale of about 100 nm (see the enlarged part).

phases.²⁸ This means that optical isotropy is due to a random microdomain structure, where the uniformly aligned smectic domains have a size which is smaller than the wavelength of light. This distorted structure makes it difficult to assign the ground-state structure to one of the four possible structures shown in Figure 1 because no aligned samples for X-ray scattering could be obtained. However, compound **Si₃-11B14** shows a temperature-dependent inversion of chirality, and this provides the possibility to make a conclusion on the structure of these dark conglomerate phases (see section 2.2.2.).

2.2.2. The Soft Crystalline Dark Conglomerate Phase of Si₃-11B14. Compound **Si₃-11B14** shows a transition from the $\text{SmC}_s\text{P}_F^{[*]}$ phase to a higher ordered low-temperature dark conglomerate mesophase at 56 °C on cooling (phase transition at 60 °C upon heating), which is accompanied by a reversible inversion of the chirality sense of the chiral domains. Bright domains in the high-temperature phase become dark in the lower temperature phase and vice versa (Figure 2a–e). Though temperature-dependent inversion of chirality has been observed for helical superstructure in chiral nematic (N^*) and chiral smectic C phases (SmC^*) of chiral molecules,²⁹ this is the first example of a temperature-dependent reversal of the optical rotation in a mesophase formed by achiral molecules. X-ray studies indicate that the layer thickness decreases from 4.4 nm in the fluid smectic phase ($\text{SmC}_s\text{P}_F^{[*]}$) to 3.7 nm in the low-temperature $\text{SmX}^{[*]}$ phase. Using the model shown in Figure 3a and assuming a bending angle of 120° ($d_{\text{model}} = 6.2 \text{ nm}$), a

tilt angle of $\theta = 43^\circ$ was calculated according to $d_{X\text{-ray}}/d_{\text{model}} = \cos \theta$ for the $\text{SmC}_s\text{P}_F^{[*]}$ phase, which is the same value as that determined by electrooptical investigations (see section 3). In the $\text{SmX}^{[*]}$ phase, the calculated tilt angle is about 53°. No additional reflections occur in the small-angle region, which indicates that this mesophase also has a layer structure. The maximum of the broad diffuse peak in the wide-angle region, however, is split into several reflections (see Figure 4, curve c), confirming an additional in-plane ordering in the low-temperature mesophase.³⁰ As no birefringence is introduced at the phase transition, the distorted nature of the smectic phase should be maintained at the phase transition. The proven tilted arrangement of the molecules distinguishes this phase from the soft crystalline $\text{B}_4^{[*]}$ phase,³¹ which is a nontilted low-temperature phase with a TGB-like helical superstructure.³²

2.2.3. Possible Structures of the Dark Conglomerate Phases. 2.2.3.A. Origin of Layer Distortion. Layer distortion in the investigated systems might arise due to a steric frustration of the areas required by the aromatic and the nonaromatic molecular parts at the interfaces, which could lead to a Gaussian curvature of these interfaces.³³ Optical isotropic bicontinuous cubic phases^{8a,c,g,9a,b,34} are known to occur as intermediate states

- (28) (a) Strey, R.; Winkler, J.; Magid, L. *J. Phys. Chem.* **1991**, *95*, 7502–7507. (b) Roux, D.; Coulon, C.; Cates, M. E. *J. Phys. Chem.* **1992**, *96*, 4174–4187. (c) Porte, G. *Curr. Opin. Colloid Interface Sci.* **1996**, *1*, 345–349. (d) Hyde, S. T. *Colloids Surf. A* **1997**, *129–130*, 207–225.
- (29) (a) Vill, V.; von Minden, H. M.; Bruce, D. W. *J. Mater. Chem.* **1997**, *7*, 893–899. (b) Langner, M.; Praefcke, K.; Krücker, D.; Heppke, G. *J. Mater. Chem.* **1995**, *5*, 693–699. (c) Kaspar, M.; Gorecka, E.; Sverenyak, H.; Hamplova, V.; Glogarova, M.; Pakhomov, S. A. *Liq. Cryst.* **1995**, *19*, 589–594. (d) Loubser, C.; Wessels, P. L.; Styring, P.; Goodby, J. W. *J. Mater. Chem.* **1994**, *4*, 71–79.

- (30) This is in line with the fact that no electrooptical switching is observed in this soft crystalline mesophase.
- (31) (a) Niwano, H.; Nakata, M.; Thisayukta, J.; Link, D. R.; Takezoe, H.; Watanabe, J. *J. Phys. Chem. B* **2004**, *108*, 14889–14896. (b) Araoka, F.; Ha, N. Y.; Kinoshita, Y.; Park, B.; Wu, J. W.; Takezoe, H. *Phys. Rev. Lett.* **2005**, *94*, 1–4. (c) Walba, D. M.; Eshdat, L.; Körblová, E.; Shoemaker, R. K. *Cryst. Growth Des.* **2005**, *5*, 2091–2099.
- (32) In principle, it is possible that also in the $\text{SmX}^{[*]}$ phase the smectic slabs might adopt a TGB-like helical organization as in the $\text{B}_4^{[*]}$ phases, but there is no indication of such a helical structure.
- (33) (a) Seddon, J. M.; Templer, R. H. *Handbook of Biological Physics*; Lipowsky, R., Sackmann, E., Eds.; Elsevier: Amsterdam, 1995; Vol. 1, pp 97–160. (b) Hyde, S. T. *Handbook of Applied Surface and Colloid Science*; Holmberg, K., Ed.; Wiley: Chichester, 2001; Vol. 2, pp 299–332.
- (34) (a) Gharbia, M.; Gharbi, A.; Nguyen, H. T.; Malthete, J. *Curr. Opin. Colloid Interface Sci.* **2002**, *7*, 312. (b) Bruce, D. W. *Acc. Chem. Res.* **2000**, *33*, 831–840.

at the transition from flat smectic layers to an organization in columns. The fact that the mesophases under discussion occur upon introduction of a bulky siloxane unit into the molecule **12B12**, itself forming a nondistorted smectic phase, and that elongation of the alkyl chains leads to the formation of columnar phases (see section 2.2.5.) would be in line with this explanation. However, a cubic lattice can be excluded for the mesophases under investigation (rather high fluidity, no X-ray evidence), and fluid isotropic intermediate phases are extremely rare in thermotropic systems and usually occur only for few homologues in limited temperature ranges.^{35,36} In contrast, the dark conglomerate phases were found over the whole temperature range for a wide variety of different compounds.^{15–18}

Sponge phases (L_3 phases) are optically isotropic mesophases which are quite common in lyotropic systems. These mesophases occur beside lamellar phases over a quite large range of dilution, if the surfactant bilayers are swollen by solvents. In these sponge phases, the layers are curved and form a continuous nonperiodic web of bilayers (Figure 3c).^{27,28} Interestingly, also the dark conglomerate phases can be found for molecules with relatively long alkyl chains or chains which are functionalized with bulky end groups (siloxanes, carbosilanes). In addition, if *n*-dodecane is added to the nonsilylated compound **12B12**, the typical birefringent schlieren texture of the $SmCP_A$ (B_2 -type) phase is completely replaced by a well developed dark conglomerate texture, similar to that shown in Figure 2a,b, and the layers are expanded from $d = 3.7$ nm for the pure compounds to $d = 3.9$ nm for the solvent-saturated sample.³⁷ Hence, a sponge-like random web of the aromatic sublayers that divides the fluid regions into homogeneous (siloxanes and alkyl chains are mixed) or inhomogeneous (siloxanes are separated from the alkyl chains) labyrinths is a likely model for the observed dark conglomerate phases (see Figure 3c).

As mentioned above, layer distortion in these sponge-like structures might result from a slight misbalance of the areas required by the incompatible segments at the interfaces. Layer distortion might also arise as a result of the escape from a macroscopic polar order if the ground-state structure is ferroelectric (SmC_sP_F or SmC_aP_F). Splay of the polar directions in SmC_sP_F layers can, for example, give rise to a regular wavy deformation of the layers which leads to the birefringent B_7 -type phases.³⁸ A nonregular deformation of polar layers in all three dimensions could give rise to a optically isotropic sponge-like structure.

In addition, chirality can also be a source of layer distortion. Chirality in self-organized superstructures, formed by achiral bent-core molecules, arises from the tilted organization of these molecules in polar layers.¹³ The $SmCP$ layers have a C_2 phase symmetry which lacks a mirror plane, and therefore, these layers are inherently chiral. Layer normal, tilt direction, and polarization vector describe either a right-handed or a left-handed system (see Figure S1 in the Supporting Information). Changing either the direction of layer polarization or the tilt direction changes the chirality sense of the layer.¹³ The SmC_sP_A and SmC_sP_F phases have opposite chirality sense in adjacent layers (see Figure 1, indicated by different color), leading to macroscopic racemic superstructures,³⁹ whereas in the SmC_aP_A and SmC_sP_F phases, the layers have identical chirality sense and hence these structures are homogeneously chiral (Figure 1). As bent-core molecules preferably adopt helical molecular conformations,^{40,41} diastereomeric relations of these chiral conformers with the layer chirality could lead to a (partial) deracemization of molecular conformations; that is, one helix sense is dominating in the (+)- SmC_sP_F domains, whereas the opposite helix sense is dominating in the (–)- SmC_sP_F domains.⁴² As chiral molecules cannot align completely parallel in soft matter systems, this conformational chirality could contribute to layer distortion.^{12c}

2.2.3.B. Origin of Optical Activity. Recently, Hough and Clark have predicted that a significant optical activity arises from the layer chirality of the polar tilted smectic phase structure.²⁰ This means that a significant optical rotation is an intrinsic property of the homogeneous chiral layer structures (FE, SmC_sP_F ; or AF, SmC_aP_A), which could only be observed if the birefringence of the mesophase is low. The unique temperature-dependent inversion of the chirality sense at the phase transition from the fluid smectic $SmC_sP_F^{[*]}$ phase to the higher ordered $SmX^{[*]}$ phase observed for compounds **Si₃-11B14** (section 2.2.2.) and **Si₃-9B12** (section 2.3.) can be satisfactorily explained by the idea of layer optical chirality. For this optical activity, the sign of the optical rotation is dependent on the tilt angle of the long axis of the bent aromatic core with respect to the layer plane,²⁰ and such a change of the tilt angle was found at this phase transition. This change in tilt angle should lead to an inversion of optical rotation as proposed by this model.

2.2.3.C. Phase Structure and Polar Order. This means that the ground-state structure of the dark conglomerate phases of the silylated compounds should be homogeneous chiral, either SmC_sP_F or SmC_aP_A , and the chiral domains of opposite handedness represent regions with a distinct sense of the layer chirality. Hence, if the correlation of the tilt direction could be determined, it would be possible to decide if the ground-state structure is either ferroelectric (synclinal tilt, SmC_sP_F) or antiferroelectric (anticlinal tilt, SmC_aP_A). However, due to the distorted structure

- (35) Optically isotropic mesophase in achiral LC: (a) Warmerdam, T. W.; Nolte, R. J. M.; Drenth, W.; van Miltenburg, J. C.; Frenkel, D.; Zijlstra, R. J. J. *Liq. Cryst.* **1988**, *3*, 1087–1104. (b) Weissflog, W.; Letko, I.; Pelzl, G.; Diele, S. *Liq. Cryst.* **1995**, *18*, 867–870. (c) Pietrasik, U.; Szydłowska, J.; Krowczyński, A.; Pociecha, D.; Gorecka, E.; Guillon, D. *J. Am. Chem. Soc.* **2002**, *124*, 8884–8890. (d) Bilgin-Eran, B.; Tschierske, C.; Diele, S.; Baumeister, U. *J. Mater. Chem.* **2005**, DOI 10.1039/b511832h. (36) Optically isotropic mesophase in chiral LC: (a) Yamamoto, J.; Nishiyama, I.; Inoue, M.; Yokoyama, H. *Nature* **2005**, *437*, 525–528. (b) Nishiyama, I.; Yamamoto, J.; Goodby, J. W.; Yokoyama, H. *Chem. Mater.* **2004**, *16*, 3212–3214. (c) Nguyen, H. T.; Ismaili, M.; Isaert, N.; Achard, M. F. J. *J. Mater. Chem.* **2004**, *14*, 1560–1566. (d) Takanishi, Y.; Ogasawara, T.; Yoshizawa, A.; Umezawa, J.; Kusumoto, T.; Hiyama, T.; Ishikawa, K.; Takezoe, H. *J. Mater. Chem.* **2002**, *12*, 1325–1330. (e) Goodby, J. W.; Dunmur, D. A.; Collings, P. J. *Liq. Cryst.* **1995**, *19*, 703–709. (37) Induction of an optically isotropic mesophase by addition of organic solvents was also reported by Jakli et al., but no chiral domain structure was observed for these mesophases and the switching was reported to be ferroelectric, which is in contrast to our observations: (a) Jakli, A.; Cao, W.; Huang, Y.; Lee, C. K.; Chien, L.-C. *Liq. Cryst.* **2001**, *28*, 1279–1283. (b) Huang, M. Y. M.; Pedreira, A. M.; Martins, O. G.; Figueiredo Neto, A. M.; Jakli, A. *Phys. Rev. E* **2002**, *66*, 031708. (38) Clark, N. A.; et al. *Science* **2003**, *301*, 1204–1211.

- (39) Concerning a discussion of the actual structure of the SmC_sP_F and SmC_aP_A phases, see: (a) Folcia, C. L.; Ortega, J.; Etxebarria, J. *Liq. Cryst.* **2003**, *30*, 1189–1191. (b) Pyc, P.; Mieczkowski, J.; Pociecha, D.; Gorecka, E.; Donnio, B.; Guillon, D. *J. Mater. Chem.* **2004**, *14*, 2374–2379. (40) (a) Osipov, M. A.; Kuball, H.-G. *Eur. Phys. J. E* **2001**, *5*, 589–598. (b) Nakata, M.; Takanishi, Y.; Watanabe, J.; Takezoe, H. *Phys. Rev. E* **2003**, *68*, 041710. (c) Gorecka, E.; Cepic, M.; Mieczkowski, J.; Nakata, M.; Takezoe, H.; Zenks, B. *Phys. Rev. E* **2003**, *67*, 061704. (41) Earl, D. J.; Osipov, M. A.; Takezoe, H.; Takanishi, Y.; Wilson, M. R. *Phys. Rev. E* **2005**, *71*, 021706. (42) It should be mentioned here that chirality might also arise from a spontaneous deracemization of molecular conformations as proposed for the $B_4^{[*]}$ phases.³¹

of these smectic phases, it is impossible to get uniformly aligned samples, and therefore, the layer correlation cannot be derived from X-ray data. As it will be shown in section 3.3., the layer distortion can be squeezed out under an electric field, leading to birefringent textures with circular domains. Viewed between crossed polarizers, these domains are characterized by dark extinction brushes (see, for example, Figure 13b,c). The tilt direction can be deduced from the position of the extinction brushes with respect to the positions of polarizer and analyzer. If these brushes are inclined with the direction of the polarizers, the tilt is synclinic, and if the brushes coincide with the directions of the polarizers, it is anticlinic. Under a DC field, only the synclinic structure is found for the smectic phases of all compounds **Si₃-11Bn** with $n = 4-16$ (see section 3.3.). If it is assumed that a DC field does not change the tilt correlation, then the ground-state structure should also be synclinic. The only homogeneously chiral structure with synclinic tilt is SmC_sP_F, and this means that the correlation of the polar directions should be ferroelectric in these smectic phases.⁴³ Hence, the escape from a macroscopic polarization in the SmC_sP_F structure might contribute to the distortion of a flat layer structure. However, it should be mentioned that in the mixed system **12B12** + dodecane, where a dark conglomerate phase is induced by the solvent, the switching remains clearly AF (two polarization current peaks in a half period of an applied triangular wave field), as in the SmCP_A (B₂) phase of the solvent free material. This confirms that formation of dark conglomerate textures is independent of polar order, and layer distortion is also found in nonpolar SmCP_A phases.^{15c-h} Therefore, it can be concluded that escape from polar order can reinforce layer distortion, but steric effects and possibly also chirality effects are also required.

2.2.4. The Undulated Smectic Phases of Si₃-11B18. The mesophases of compound **Si₃-11B18** are distinct from the lower homologues. On cooling, at 104 °C, spherulitic and lancet-like textures as are typical for a mesophase with 2D lattice (Figure 7a) were observed.^{18h,j,44,45} On further cooling, at 96 °C, a phase transition takes place, the texture becomes broken, and a fluid fine schlieren texture is formed (Figure 7b). However, X-ray investigation indicates a layer structure with $d = 4.4$ nm at all temperatures (Figure 8a). The absence of the diffuse scattering around $D = 0.7$ nm of the oligosiloxane sublayers (see Figure 4, curve b) proves a nonsegregated structure where oligosiloxane units and alkyl chains are mixed up, and the unsymmetrical profile of the wide-angle scattering in the aligned sample⁴⁶ (higher intensity at the right, see Figure 8a) indicates a synclinic organization with an extremely large tilt angle ($\theta \approx 49^\circ$).

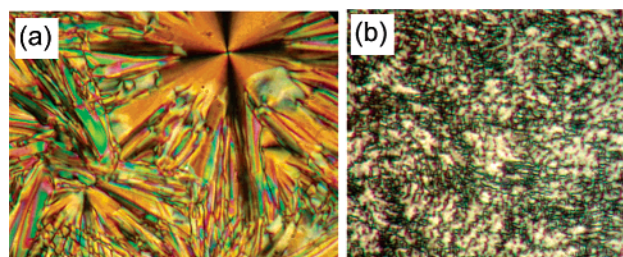


Figure 7. Textures of compound **Si₃-11B18** as seen between crossed polarizers; (a) USmC_sP_F phase at 106 °C, as obtained by cooling from the isotropic liquid; (b) USmC_sP_F phase at 90 °C as obtained by cooling from the USmC_sP_F phase.

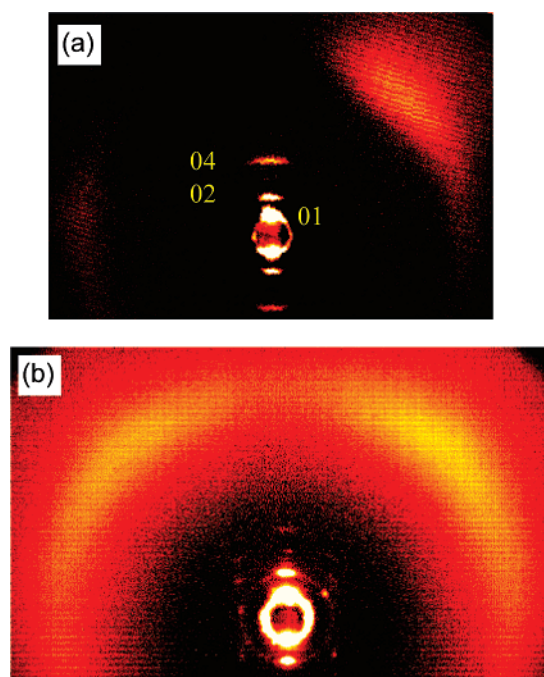


Figure 8. X-ray diffraction pattern of aligned samples. (a) USmC_sP_F phase of compound **Si₃-11B18** at 85 °C (the 03 reflection is very weak); the diffraction pattern does not change at the transition to the USmC_sP_F phase; (b) ColobP_A phase of **Si₃-11B22** at 97 °C; in both cases, the stronger intensity of the wide-angle scattering on the right is indicative of a synclinic tilt of the molecules; in (b), synclinic domains with opposite tilt direction coexist, and therefore, a wide-angle scattering is also found on the left; the distinct intensity of these scatterings indicates a synclinic organization, but if both would have the same intensity, a synclinic or anticlinic tilted organization could not be distinguished.

Though a phase transition can be detected at 96 °C by a significant change of the texture and by a peak in the DSC ($\Delta H = 1.8$ kJ mol⁻¹), no change was found at this temperature in the X-ray diffraction pattern. This means the organization is synclinic in both mesophases. In addition, the layer reflections are extended to lines parallel to the equator in both phases (see Figure 8a), which points to mesophases with a wavy deformed (undulated) layer structure, as shown in Figure 9b.^{38,45} The difference between these two phases might arise from a different undulation wavelength and a different correlation length of the undulations in adjacent layers. In the smectic-like low-temperature phase (USmC_sP_F), there might be only a short-range correlation of the undulations, whereas in the high-temperature phase (USmC_sP_F), the correlation might become medium or long range, leading to a change of the optical appearance of the mesophase from a smectic-like texture to a texture more reminiscent of a mesophase with 2D lattice.

- (43) In addition, a synclinic organization of the molecules was proven for the undulated variants of the smectic phase (compound **Si₃-11B18**) by X-ray scattering of aligned samples (see Figure 8a).
- (44) Examples of columnar phases formed by bent-core molecules: (a) Watanabe, J.; Niori, T.; Sekine, T.; Takezoe, H. *Jpn. J. Appl. Phys.* **1998**, *37*, L139-L142. (b) Mieczkowski, J.; Gomola, K.; Koseska, J.; Pociecha, D.; Szydłowska, J.; Gorecka, E. *J. Mater. Chem.* **2003**, *13*, 2132-2137. (c) Amarathana Reddy, R.; Sadashiva, B. K.; Raghunathan, V. A. *Chem. Mater.* **2004**, *16*, 4050-4062. (d) Pelz, K.; Weissflog, W.; Baumeister, U.; Diele, S. *Liq. Cryst.* **2003**, *30*, 1151-1158. (e) Kardas, D.; Prehm, M.; Baumeister, U.; Pociecha, D.; Amarathana Reddy, R.; Mehl, G. H.; Tschierske, C. *J. Mater. Chem.* **2005**, *15*, 1722-1733. (f) See ref 21b. (g) Nguyen, H. T.; Bedel, J. P.; Rouillon, J. C.; Marcerou, J. P.; Achard, M. F. *Pramana J. Phys.* **2003**, *61*, 395-404.
- (45) Keith, C.; Amarathana Reddy, R.; Baumeister, U.; Tschierske, C. *J. Am. Chem. Soc.* **2004**, *126*, 14312-14313.
- (46) These mesophases are distinct from the dark conglomerate phases of the lower homologues, and therefore, aligned samples can be obtained.

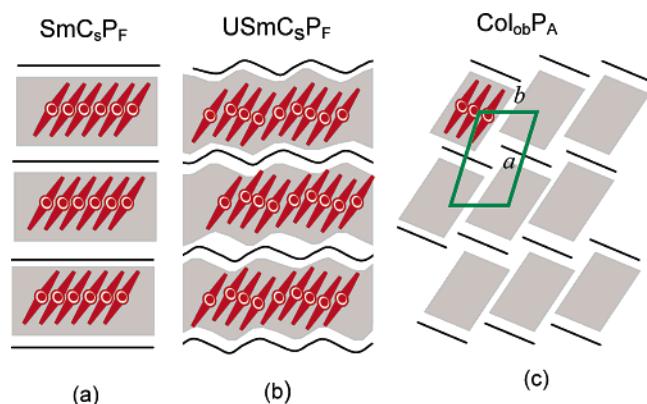


Figure 9. Possible way for the transition from (a) a smectic phase via (b) a nonsinusoidal undulated smectic phase (wavy deformed layers, the undulation period can be much larger than actually shown) to (c) an oblique columnar phase (broken layers, the resulting ribbons are organized in an oblique lattice) as observed with increasing steric frustration. The transition from wavy deformed layers to broken layers is associated with a change of the polar order from ferroelectric to antiferroelectric. The possibilities concerning the polar directions in the Col_{ob}P_A phase are discussed in Figure S6, Supporting Information.

2.2.5. The Undulated Smectic and Columnar Phases of Si₃-11B20 and Si₃-11B22. The textural features of the mesophases of compounds **Si₃-11B20** and **Si₃-11B22** (see, for example, Figure S5, Supporting Information) are identical with those seen for the high-temperature phase of **Si₃-11B18**.⁴⁷ The diffraction pattern of an aligned sample of compound **Si₃-11B22** is shown in Figure 8b as an example. The small-angle reflections can be indexed to an oblique columnar phase with the lattice parameters $a = 4.9$ nm, $b = 2.2$ nm, and an oblique angle $\gamma = 100^\circ$. Within this mesophase, the organization is synclitic (different intensity of the wide-angle reflections) and the tilt angle is 50° . A model of this mesophase is shown in Figure 9c. Accordingly, the layers are broken into ribbons (modulated layers), and these ribbons are organized into an oblique 2D lattice. This phase is assigned as columnar oblique (Col_{ob}). From switching experiments (see section 3.4.), it can be concluded that the organization of the molecules in adjacent ribbons is antipolar. There are at least three possible structures depending on the polar direction in adjacent ribbons, which are discussed in more detail in ref 12c and in Figure S6 of the Supporting Information.

The diffraction pattern of **Si₃-11B22** is the same in the whole temperature region, but for compound **Si₃-11B20**, there is a change of the diffraction pattern at 96°C . At higher temperature, the small-angle diffraction pattern is indicative of a Col_{ob}P_A phase ($a = 4.5$ nm, $b = 2.2$ nm, and $\gamma = 103^\circ$, Figure S7a) as in the case of **Si₃-11B22**. Around 96°C , all out-of-meridian reflections completely disappear, indicating a smectic structure until crystallization (see Figure S7b, Supporting Information). No change can be observed in the wide-angle region, indicating a synclitic tilt of the molecules in both mesophases. The diffraction pattern of this low-temperature phase is identical with the mesophase(s) of **Si₃-11B18** (layer reflections are extended

to lines), indicating a USmC_sP_F phase. As the organization of the molecules is synclitic in the undulated layer structures, the undulations should not be sinusoidal (symmetric), but asymmetric (see Figure 9b), as in the asymmetric ripple phases of phospholipids.⁴⁸

Hence, as shown in Figure 9a–c, elongation of the alkyl chains leads to a stepwise transition from dark conglomerate phases (SmC_sP_F*, **Si₃-11Bn** with $n = 4$ –16) via undulated layers (USmC_sP_F and USmC_sP_F mesophases of **Si₃-11B18** and low-temperature phase of **Si₃-11B20**) to a ribbon phase built up by fragmented layers (Col_{ob}P_A, high-temperature phase of **Si₃-11B20** and compound **Si₃-11B22**).

2.3. Effect of the Length of the Spacer Unit. The influence of the length of the aliphatic spacer unit between the bent-core and the oligosiloxane unit was investigated for the series of dodecyloxy-substituted compounds **Si₃-mB12** ($m = 5$ –11; see Table 3). Only smectic phases were found in this series. It can be clearly seen that reduction of the spacer length gives rise to a reduction of the mesophase stability, but also the textures are slightly different. Optical isotropic mesophases composed of chiral domains were observed for all homologues with relatively long spacer units with $m \geq 9$, whereas the homologues with shorter spacers ($m = 6$ –8) are characterized by the coexistence of this dark conglomerate texture and a birefringent schlieren texture (see Figure S8 in the Supporting Information). Depending on the conditions (cooling rate, type of glass surfaces, etc.), the birefringent regions can be dominating or minor. In the X-ray diffraction pattern, a diffuse scattering with a shoulder at $D = \text{ca. } 0.7$ nm (siloxane sublayers) is observed for compounds **Si₃-mB12** with $n = 7$ –11, whereas this shoulder is absent for **Si₃-6B12**. In addition, there is a remarkable and unique dependence of the layer spacing on the length of the spacer unit. Upon reduction of the spacer length, the layer spacing decreases first from $d = 4.4$ nm ($m = 11$) to $d = 3.8$ nm ($m = 7$) as expected, but for **Si₃-6B12**, it strongly rises again, so that this compound has a larger layer distance ($d = 4.8$ nm) than that of **Si₃-11B12** with seven additional CH₂ groups ($d = 4.4$ nm; see Table 3 and Figure 5). It seems that for compound **Si₃-6B12** the thin sublayers of the alkyl spacers cannot accommodate the relatively long terminal chains. The segregation of the siloxane units is lost, and these units become randomly distributed within the aliphatic sublayers of the alkyl chains, as indicated in the X-ray diffraction pattern by the complete absence of the shoulder at 0.7 nm corresponding to the oligosiloxane sublayers (see Figure S9 in the Supporting Information). As the limitation for the expansion of the aliphatic sublayers is removed, also the tilt of the aromatic cores is reduced and both effects contribute to the huge layer expansion from **Si₃-7B12** to **Si₃-6B12**.

It is remarkable that also in the homologous series of compounds **Si₃-mB12** there is one compound (**Si₃-9B12**) which shows a transition to a higher ordered low-temperature phase (see Figure S10 in the Supporting Information) with an inversion of chirality at the phase transition, very similar to that of compound **Si₃-11B14**. The neighboring homologues **Si₃-8B12** and **Si₃-10B12** do not show this type of low-temperature phase. Remarkably, the ratio of end chain length to spacer length is

(47) Though a synclitic organization in the Col_{ob}P_A and USmC_sP_F phases is clearly proven by X-ray scattering, in the textures, the extinction crosses coincide with the positions of polarizer and analyzer (see Figure S5). This indicates that these 2D-modulated smectic phases preferably adopt an alignment of the ribbons with the polarization vector parallel to the glass surfaces, which cannot be distinguished from an anticlinic organization by optical methods. See: Gorecka, E.; Vaupotic, N.; Pociecha, D.; Cepic, M.; Mieczkowski, J. *ChemPhysChem* **2005**, *6*, 1087–1093.

(48) (a) MacKintosh, F. C. *Curr. Opin. Colloid Interface Sci.* **1997**, *2*, 382–387. (b) Katsaras, J.; Tristram-Nagle, S.; Liu, Y.; Headrick, R. L.; Fontes, E.; Mason, P. C.; Nagle, J. F. *Phys. Rev. E* **2000**, *61*, 5668–5677. (c) Sengupta, K.; Raghunathan, V. A.; Katsaras, J. *Phys. Rev. E* **2003**, *68*, 031710.

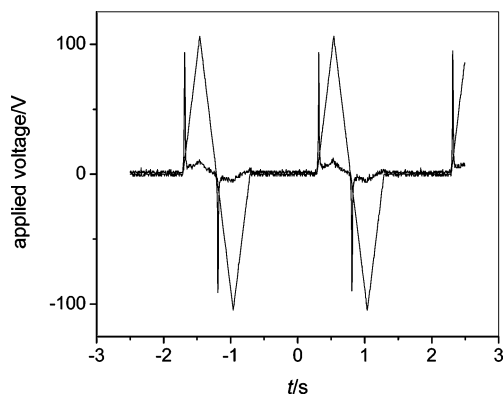


Figure 10. Switching current response of compound **Si₃-11B4** in a 6 μm polyimide-coated ITO cell (± 105 V, 1 Hz, 5 k Ω) on applying an alternating simple (regime of the downward current peak) and modified triangular wave voltage (regime of the upward current peak/s) at $T = 85$ $^{\circ}\text{C}$.

the same in both compounds (ratio = 1.3). Also, for compound **Si₃-9B12**, the layer distance decreases from $d = 4.0$ nm in the $\text{SmC}_s\text{P}_F^{[*]}$ phase to $d = 3.0$ nm in the $\text{SmX}^{[*]}$ phase, indicating an increase of the tilt angle from ca. 44 to ca. 58° . It seems that, for this special ratio of spacer length to end chain length, the terminal chains can be accommodated between the aliphatic spacer units in such a way that optimal space filling is possible if the aromatic cores adopt a strongly tilted organization in layers. This dense packing might allow the crystallization of the aromatic and possibly also of the aliphatic parts, whereas the oligosiloxane units seem to remain in a more disordered state, which retains some softness of this smectic mesophase.

3. Electrooptical Investigations. Switching experiments in electric fields can give information concerning the organization of the molecules with respect to their polar direction.¹³ All fluid smectic phases of compounds **Si_n-mBn** show only one very sharp single current peak in the half period of a triangular wave voltage, also at low frequencies (down to 1 to 0.1 Hz).⁴⁹ The calculated polarization values are between 700 and 800 nC cm^{-2} in all cases. This single peak is a first indication of a FE switching process, but this is not an unambiguous proof of ferroelectricity. For example, if the relaxation to the AF ground state would be slow, then the two polarization current peaks of an AF switching can merge to only one. Therefore, it was proposed to use a modified triangular wave field, where a delay is introduced at zero voltage.^{18c} Also under these conditions, using noncoated ITO cells,⁵⁰ independent of the temperature and cell thickness (5 or 10 μm), only one peak is observed in the modified triangular wave field (see Figure 10). This indicates that a bistable switching takes place, and that switching always occurs after zero-voltage crossing of the applied field.

Additional information was gained from the optical investigation of the switching process. Increasing the voltage of an applied electric field gives rise to a significant change of the appearance of the smectic mesophases of the silylated compounds. In the virgin ground states, most smectic mesophases

of compounds **Si_n-mBn** are optically isotropic and composed of domains of opposite chirality sense. However, above a certain threshold voltage, the texture becomes strongly birefringent. Also cooling from the isotropic liquid state under an applied electric field with a certain threshold strength leads to strongly birefringent textures with circular domains (see, for example, Figure 11a,e). This means that under an electric field the strongly distorted layer structures of the dark conglomerate phases are transformed into nearly nondistorted layers. A probable explanation could be that the alignment force provided by the electric field above a certain threshold is stronger than the layer distorting forces. More generally speaking, the structure of the mesophase investigated in the electric field experiments is distinct from the mesophase formed without applied field.

3.1. Surface-Stabilized (Metastable) Ferroelectric Switching. For the optical investigation of the switching process, circular domains were grown by slow cooling under a DC field. Within the obtained domains, the layers are aligned perpendicular to the cell surfaces (bookshelf geometry), and these layers are circularly arranged around the centers of these domains. Hence, the molecules are organized parallel to the cell surfaces. The characteristic features of these domains are extinction brushes, where the direction of the brushes are parallel and perpendicular to the direction of the optical axis of the smectic layers. The change of the position of these brushes, depending on the applied voltage, gives information about the change of the direction of the optical axes and hence about the reorganization of the molecules under the influence of the electric field.^{13a} Different types of switching behavior were observed, depending on the structure of the molecules, though only one current-response peak was observed in all cases.

For compounds **Si₃-mBn** with dark conglomerate phases ($m = 7-11$ and $n = 12$ or $m = 11$ and $n = 4-16$) under an applied DC field, circular domains were obtained, in which the extinction crosses are inclined with polarizer and analyzer, indicating a synclitic FE organization (see Figure 11a). The extinction crosses of these homogeneously chiral circular domains do not relax at zero voltage (see Figure 11b); they change their position only after application of the opposite voltage (Figure 11c). This indicates a bistable switching process (only two distinct states at + voltage and at - voltage can be observed). As also shown in Figure 11a-c, the texture of compound **Si₃-11B4** at zero voltage has nearly the same birefringence as the textures under the field. However, the birefringence slowly decreases after terminating the field, and after 30 min, the texture has become completely dark in most parts of the sample, as shown in Figure 11d. This texture is reminiscent of the virgin dark conglomerate texture, obtained by cooling from the isotropic phase without applied field, with the difference that no chiral domains could be identified (probably these domains are too small to be visible). This indicates that the switching process itself is ferroelectric, but the field-induced FE states (SmC_sP_F) are metastable at zero voltage and, on a longer time scale, relax to the macroscopically nonpolar (disordered) ground-state structure. For compound **Si₃-11B8**, the relaxation takes about 1 h, and for the long chain compounds **Si₃-11Bn** ($n = 12-16$), it cannot be observed, even after prolonged storage. Hence, the FE states, once formed in an electric field, are stabilized by surface interactions (surface stabilized FE switching).

(49) In some cases, under special conditions, the single peak can be split into two very close fused peaks, though optical investigations exclude an AF switching (see, for example, Figure S11). Probably, this is due to the coexistence of diastereomeric (energetically different) SmC_sP_F and SmC_aP_F states in these cases. It is also possible that this splitting results from an energetic difference for the molecules in the center of the sample and at the surfaces.

(50) In polyimide-coated cells, the switching behavior can be more complex in some cases, due to the effect of an induced electric double layer, which will be discussed in detail in a separate paper.

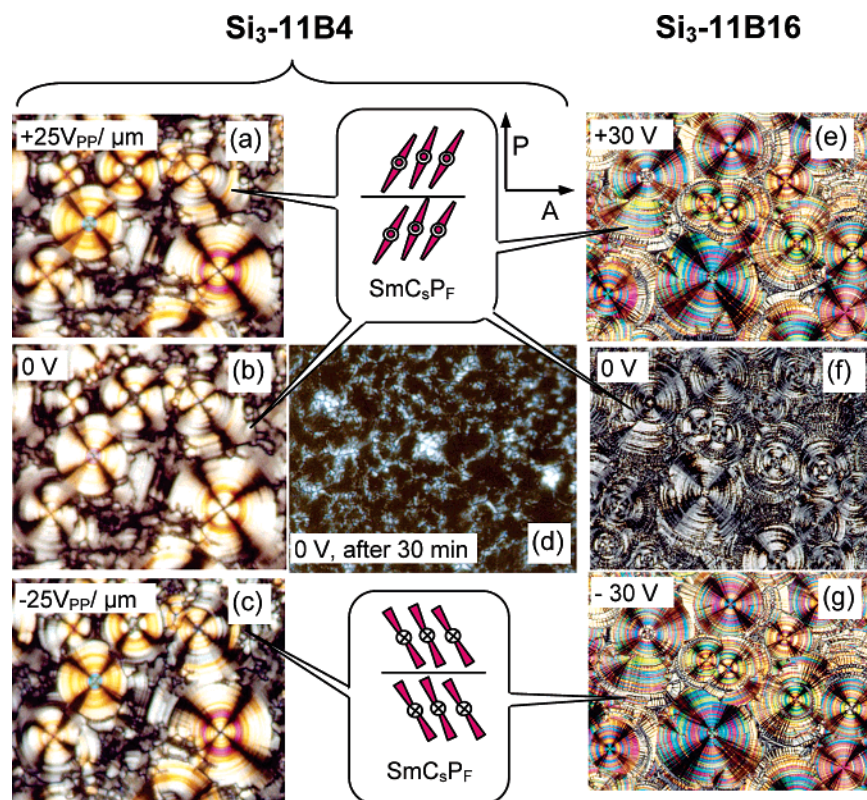


Figure 11. (a–c) Bistable (FE) switching of homogeneous chiral domains of the SmC_sP_F phase of compound **Si₃-11B4** (crossed polarizers, indicated by arrows, $T = 100\text{ }^\circ\text{C}$, $6\text{ }\mu\text{m}$, polyimide-coated ITO cell, 1 Hz); (d) texture obtained after terminating the applied field for about 30 min; (e–g) switching process of the polar smectic phase of compound **Si₃-11B16** ($T = 105\text{ }^\circ\text{C}$, $6\text{ }\mu\text{m}$ polyimide-coated ITO cell).

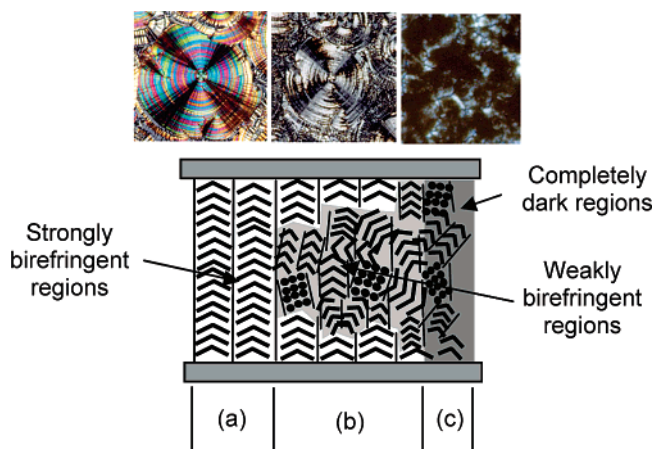


Figure 12. Organization of bent-core molecules in the ITO cell at zero voltage after removal of the field: (a) the position of the extinction brushes and the birefringence of the texture remain after switching off the electric field (compound **Si₃-11B4**) due to the robust layer structure; (b) the texture becomes weakly birefringent due to the disordered structure in the center, and the position of the extinction crosses is not changed, due to surface coupling; (c) optically isotropic regions, where throughout the whole sample the smectic layers are distorted in such a way that the ferroelectric clusters are disordered (weak coupling to the surface).

3.2. Combined Surface-Stabilized FE Switching and Superparaelectric Switching. With increasing chain length, the optical appearance of the zero-voltage state changes. This is most clearly seen for compound **Si₃-11B16** (see Figure 11e–g). Here the birefringence significantly drops after switching off the field, though the direction of the extinction crosses does not change; that is, the organization should remain synclinic and therefore should remain highly birefringent. This reduction

of birefringence during switching can be observed for all apparently bistable switching smectic phases of the series **Si₃-11Bn**. It is only marginal for **Si₃-11B4** (see Figure 11a–c), and it becomes stronger with increasing chain length and is the strongest for **Si₃-11B16**. It seems that immediately after switching off the electric field in the center of the sample the flat smectic layers become distorted (optically isotropic), as in the ground-state structure. Only at the surfaces do the nondistorted (birefringent) layers remain. In these surface layers, the position of the extinction crosses is retained. This indicates that the SmC_sP_F structure is stabilized due to surface alignment, and these surface layers switch into the other polar state after field reversal. In the field-on state, the disordered layer fragments in the center reorganize into the configuration defined by the surface layers, and the texture becomes highly birefringent again. It seems that the degree of coupling between the molecules with respect to the strength of the surface anchoring is responsible for the chain length dependence of this effect (see Figure 12). If the layers are robust (short alkyl chains), the surface-stabilized polar structure is stable in the whole sample for a certain period of time. However, the coupling to the surfaces is not strong enough to maintain the polar order after switching off the electric field, and hence, in the whole sample, the polar layers slowly relax to the macroscopically apolar dark conglomerate structure (see Figure 12c). If the coupling between the molecules is weak (long alkyl chains), then a significant amount of the material immediately relaxes and only thin surface layers remain (see Figure 12b). Because in this case the coupling between the molecules within the smectic phase is weaker than anchoring to the surfaces, the texture within the surface layers is stable

and is not affected by the relaxation of the majority of the material into the optical isotropic disordered structure.

Hence, for compounds **Si₃-11Bn** with $n = 6-16$, the switching process is not classical ferroelectric, where one macroscopically polar state switches directly into another one with opposite polarity. This process can only be seen at the surfaces where the ferroelectric domains are stabilized by surface alignment (surface-stabilized FE switching). In the center (where the influence of the surfaces is weak), the polar layers are unstable and relax into smaller ferroelectric domains which adopt a random orientation in space (as in the dark conglomerate ground-state structure). This model is similar to that suggested for a superparaelectric switching process.⁵¹ These investigations confirm that the ground-state structure is ferroelectric (SmC_sP_F) and the disordered (optically isotropic) structure allows an escape from the macroscopic polar order. In other words, though the local microstructure is polar, the mesophase itself is macroscopically apolar.

3.3. The Field-Induced Smectic Phases of Si₃-11B18: At the Borderline to AF Switching. Also for compound **Si₃-11B18** with an octadecyl terminal chain, only one peak was observed for the switching under a triangular wave field. This type of current response was found in the whole mesomorphic temperature range, that is, in the temperature range of both undulated smectic mesophases ($\text{USmC}_s\text{P}'_F$ and USmC_sP_F). However, it must be considered that under the influence of the electric field the layer undulation is squeezed out, as the texture is different from the ground-state structure and identical to those observed for flat layer structures.^{52,53} In addition, the phase transition at 96 °C cannot be observed in the field-aligned samples. This means that the actually investigated mesophase is not one of the undulated USmC_sP_F phases, but a field-induced nonundulated smectic phase. Nevertheless, the switching process observed under the polarizing microscope indicates some significant differences to those observed for the smectic phases of the other compounds **Si₃-11Bn** with shorter chains ($n = 4-16$). As shown in Figure 13b, on cooling under a triangular wave AC field, only domains with extinction brushes parallel to analyzer and polarizer could be observed, as usually seen for anticlinic tilted smectic phases.⁵⁴ However, the textural changes seen during switching of these domains are distinct from those usually observed for typical anticlinic domains of classical bent-core molecules.^{13a} To explain this observation, it is assumed that the fundamental structure is still SmC_sP_F , but there are additional synpolar (P_S) and anticlinic interfaces. Due to these SmC_aP_S interfaces, the tilt direction between adjacent synclinc ferroelectric (SmC_sP_F) domains (stacks of layers) alternates. The size of the domains is smaller than the wavelength of light, and therefore, the extinction brushes coincide with the direction of polarizer and analyzer (see Figure 13b). At high temperature (Figure 13a), on terminating the applied field, no change in the position of the extinction brushes could be seen, except for a significant decrease in the birefringence. As mentioned earlier, this reduction of the birefringence can be explained by the

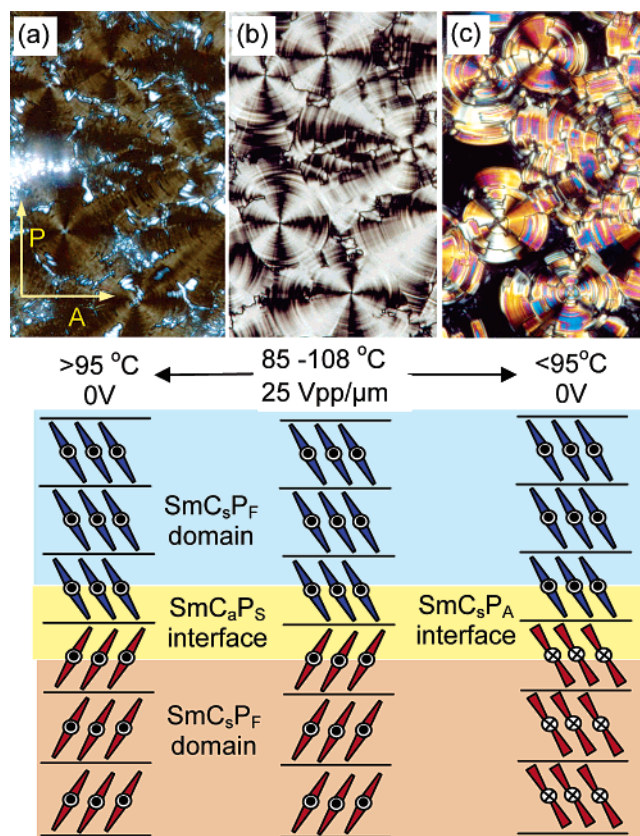


Figure 13. Temperature dependence of the switching process of compound **Si₃-11B18**, (b) under the applied AC field (6 μm polyimide-coated ITO cell, 25 $\text{V}_{\text{pp}}/\mu\text{m}$, $f = 1$ Hz); (a) after switching off the field at $T > 95$ °C, the position of the dark extinction brushes does not change (FE state is stable at the surfaces and in the center of the cell relaxes to a dark conglomerate phase); and (c) after switching off the field at $T < 95$ °C, in the bright regions the dark brushes become inclined with respect to polarizer and analyzer (the FE state relaxes to the AF ground state by rotation on a cone); in the dark regions, the texture is the same as in (a); the models below show sections of the proposed microdomain structures composed of SmC_sP_F domains with synpolar and anticlinic interfaces in (a) and (b) and with antipolar and synclinc interfaces in (c); to avoid confusion the terms synpolar (subscript S) and antipolar (subscript A) are used to characterize the polar correlation between domains, whereas the polar correlation between the individual layers is described as ferroelectric (= synpolar) and antiferroelectric (= antipolar).

formation of a dark conglomerate structure in the center of the sample (SmC_sP_F domains become disordered and escape from the macroscopic polar order), whereas the polar structure at the cell surfaces remains. Hence, the switching is surface-stabilized FE plus superparaelectric.

At the temperature where a phase transition is optically observed in the ground-state structure, a change of the switching behavior is also observed in the field-induced smectic phase. Upon termination of the field at low temperature (Figure 13c), the extinction brushes slowly relax with rotation to positions inclined with the directions of polarizer and analyzer, and the birefringence strongly increases in the zero-voltage state. This clearly indicates a relaxation to a ground-state structure, in which the synclinc domains adopt a uniform tilt direction. The relaxation takes place on a cone and leads to a synclinc and antipolar (P_A) organization of the SmC_sP_F domains with discrete SmC_sP_A boundaries between them, yielding a total nonpolar ground-state structure, as shown in the lower part of Figure 13c. The antipolar organization of the domains removes a main

(51) Achard, M. F.; Bedel, J. Ph.; Marcerou, J. P.; Nguyen, H. T.; Rouillon, J. C. *Eur. Phys. J. E* **2003**, *10*, 129–134.

(52) Examples of field-induced Col to Sm transitions: (a) Ortega, J.; de la Fuente, M. R.; Etxebarria, J.; Folcia, C. L.; Diez, S.; Gallastegui, J. A.; Gimeno, N.; Ros, M. B. *Phys. Rev. E* **2004**, *69*, 011703. (b) Etxebarria, J.; Folcia, C. L.; Ortega, J.; Ros, M. B. *Phys. Rev. E* **2003**, *67*, 042702.

(53) Such a change of the mesophase structure was also observed for B₇-type phases; see ref 38.

(54) Provided that the layers are organized in a bookshelf geometry; see ref 47.

driving force for layer distortion, giving rise to a nondistorted and therefore highly birefringent texture. It should be mentioned that not the whole sample adopts this synclinc antipolar SmC_sP_F domain structure. The dark areas, seen in Figure 13c, represent regions with the same low birefringent texture as shown in Figure 13a (with an anticlinic synpolar organization of the SmC_sP_F domains in the surface layers). Hence, the switching process seems to be metastable ferroelectric, with two distinct relaxation mechanisms. One of them leads to a distorted layer structure (superparaelectric type of switching combined with surface-stabilized FE switching), the other one to nondistorted layers with synclinc antipolar SmC_sP_A interfaces between the SmC_sP_F domains. The latter one can be regarded as a nonclassic type of AF switching (reorientation of FE domains, which is distinct from the AF switching of the B_2 -type SmCP_A phases, where every second layer is switched).⁵⁵

The same switching behavior as observed for **Si₃-11B18** was also found for compounds **Si_x-11B12** with short silicon-containing units ($x = 1$ or 2 ; see Figure S12 in the Supporting Information) and compounds **Si₃-mB12** with short spacer units ($m = 5$ and 6), that is, it is found for all compounds forming smectic phases without discrete siloxane sublayers, where alkyl chains and siloxane units are mixed in common sublayers (and the diffuse wide angle scattering at $D = 0.7$ nm is missing).

The stepwise change of the organization of the molecules and their switching behavior can be understood by a continuous transition from a discrete triple layer organization to a simple layer structure composed of only two types of sublayers. Compounds with discrete siloxane sublayers have a strong preference for the SmC_sP_F structure under all conditions. For silylated compounds without these siloxane sublayers, where the siloxane groups are organized in common layers with the alkyl chains, the stability of the ferroelectric structure is reduced, so that also antipolar interfaces can emerge, but the SmC_sP_F structure is still dominating. This reduction of segregation also leads to a change of the textures from the purely dark conglomerate type ($\text{SmC}_s\text{P}_F^{[*]}$) to a coexistence of birefringent and dark conglomerate textures ($\text{SmC}_s\text{P}_F^{[*/*]}$). For compounds **En-9Bn** and **12B12** without siloxane units, the SmC_sP_F stabilizing effect is completely missing in the ground state, and for these compounds, antiferroelectric ground-state structures are strongly favored, leading to birefringent textures and classical AF switching under all conditions.

3.4. The AF Switching $\text{Col}_{ob}\text{P}_A$ Phase of Compound **Si₃-11B22: Switching of Superstructural Chirality.** For compound **Si₃-11B22**, which shows exclusively the $\text{Col}_{ob}\text{P}_A$ phase, the switching process is clearly AF as indicated by the presence of two well separated repolarization current peaks (see Figure 14). The value of the spontaneous polarization ($350\text{--}400$ nC cm^{-2}) is significantly smaller than that in the smectic phases.⁵⁶ The extinction crosses are always inclined with the directions of polarizer and analyzer, and this indicates that the synclinc organization of the ground-state structure (see section 2.2.5.)

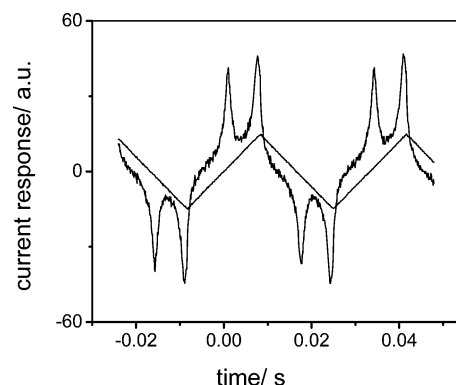


Figure 14. Switching current response of the $\text{Col}_{ob}\text{P}_A$ phase of compound **Si₃-11B22** in a $5\text{ }\mu\text{m}$ noncoated ITO cell (± 150 V, 20 Hz) at $T = 90^\circ\text{C}$.

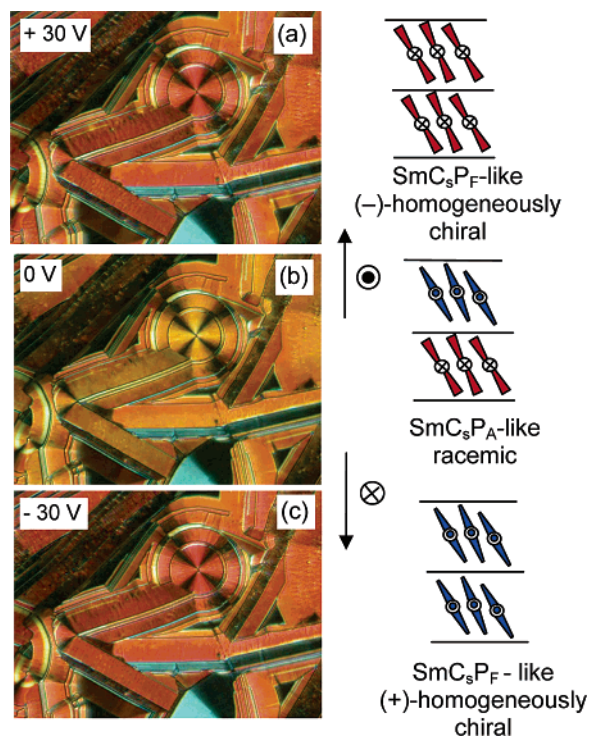


Figure 15. Switching process of the polar $\text{Col}_{ob}\text{P}_A$ phase of compound **Si₃-11B22** ($5\text{ }\mu\text{m}$ noncoated ITO cell), as seen between crossed polarizers ($T = 90^\circ\text{C}$); the position of the extinction cross does not change, only the birefringence slightly decreases in the zero-field state, which indicates a switching around the long axis.

is not significantly changed by the field (Figure 15). The layer modulation remains under the electric field, as can be seen by the textures of the field-aligned samples (Figure 15), which are very different from those typically observed for the smectic phases. Because of the modulation of the layers, the switching on a cone is restricted by the inter-ribbon boundaries, and therefore, the switching takes place around the long axis as is typical for $\text{Col}_{ob}\text{P}_A$ phases.^{45,57} Indeed, in the circular domains,

(55) The observation of only a single peak in switching experiments under a triangular wave field might be due to the fact that the relaxation to the synclinc antipolar organization (nonclassic AF switching) is slow. Hence, under a triangular AC field, the synclinc antipolar boundaries, seen in DC field experiments, cannot be formed to a considerable extent, possibly because the anticlinic defects in the surface layers inhibit the fast reorganization to a purely synclinc structure.

(56) In addition, the threshold voltage (~ 50 V_{pp}/μm) is much higher than that for the smectic phases (**Si₃-11B4** ~ 16 V_{pp}/μm to **Si₃-11B16** ~ 7 V_{pp}/μm, USmC_sP_F phase of **Si₃-11B16** ~ 30 V_{pp}).

(57) Examples for switching of suprastructural chirality by collective rotation around the long axis: (a) Schröder, M. W.; Diele, S.; Pelzl, G.; Weissflog, W. *ChemPhysChem* **2004**, *5*, 99–103. (b) Szydłowska, J.; Mieczkowski, J.; Matraszek, J.; Bruce, D. W.; Gorecka, E.; Pociecha, D.; Guillon, D. *Phys. Rev. E* **2003**, *67*, 031702. (c) Amaranatha Reddy, R.; Schröder, M. W.; Bodyagin, M.; Kresse, H.; Diele, S.; Pelzl, G.; Weissflog, W. *Angew. Chem., Int. Ed.* **2005**, *44*, 774–778. (d) Weissflog, W.; Dunemann, U.; Schröder, M. W.; Diele, S.; Pelzl, G.; Kresse, H.; Grande, S. *J. Mater. Chem.* **2005**, *15*, 939–946.

where the extinction brushes are inclined with polarizer and analyzer (synclinic domains), the position of the extinction crosses does not change, neither on terminating the field nor on reversing the field. This confirms a switching by rotation around the long axis, which changes the polar direction without changing the tilt direction of the molecules.⁴⁵ It should be noted that this switching process gives rise to a change of the superstructural chirality of the ribbons from racemic at zero voltage to homogeneously chiral under the applied field, and the change of the sign of the applied field switches between the enantiomeric chiral states (see Figure 15).^{45,57}

The high-temperature Col_{ob}P_A phase of compound **Si₃-11B20** shows the same behavior as the Col_{ob}P_A phase of **Si₃-11B22**, but for this compound, the switching process changes at the phase transition (96 °C) to the low-temperature USmC_sP_F phase, where one of the two peaks disappears. In this low-temperature mesophase, the switching behavior is essentially the same as in the field-induced smectic phases of **Si₃-11B18**. Hence, in this compound, there is a temperature-dependent change from surface stabilized FE switching (on a cone) at lower temperature to AF switching (around the long axis) at higher temperature.⁵⁸

Summary and Conclusion

The self-organization of bent-core molecules was modified in a systematic way by introduction of polyphilicity, provided by silicon-containing units, which are incompatible with the aromatic cores and the alkyl chains. Segregation of the siloxane and alkyl segments takes place if the oligosiloxane units have a sufficient length. This leads to a triple layer structure, where spacer length, length of the rigid bent core, and the size of the oligosiloxane units determine the layer spacing. If spacer length and length of the terminal alkyl chain are very different, then the end chains cannot be accommodated completely in the aliphatic regions, which disturbs segregation and gives rise to a simple layer structure where only the aromatic and nonaromatic segments are segregated. The incompatibility of the oligosiloxane units with the aromatic cores and the aliphatic chains is thought to be due to the high flexibility and the more spherical average shape of these units. Hence, related effects were observed with molecules, where carbosilane units replace the siloxane units.^{17d}

Segregation of alkyl chains and siloxane units significantly changes the mesophase structure and the switching behavior. In the ground-state structure, the synclinic ferroelectric organization of the molecules is favored (SmC_sP_F). The escape from macroscopic polar order in such mesophases contributes to a collapse of flat layers with formation of an optically isotropic microdomain structure (SmC_sP_F^[*]). In this optically isotropic mesophase, the superstructural layer chirality of the homogeneously chiral SmC_sP_F structure can be observed by an optical activity of the distinct domains (dark conglomerate phase). The observation of a change of the sense of optical rotation by changing the orientation of the aromatic cores with respect to the layer plane at the phase transition of SmC_sP_F^[*] to SmX^[*] from ca. 43–44 to ca. 52–58° can be explained on the basis of the recently suggested concept of layer optical chirality²⁰ in these polar smectic phases. This is a new source of optical activity in supramolecular systems, distinct from helical superstructures.

With increasing segregation of the oligosiloxane sublayers, the switching process changes from a classical AF-type for the nonsilylated compounds (e.g., **12B12**) via a nonclassical AF and superparaelectric switching to long-living surface-stabilized FE for the triple layer phases. The effect of the additional oligosiloxane sublayers seems to be largely entropic. Usually, the AF organization in the liquid crystalline phases of bent-core molecules allows an easy fluctuation of the molecules from layer to layer because the wings of the bent cores are organized in a synclinic fashion at the interlayer interfaces (see Figure 1). These fluctuations are more difficult in the FE structures, where the wings of the bent cores are organized in an anticlinic fashion at these interfaces and hence disturb these fluctuations. This leads to an entropic penalty for the FE structure. Because the isotropic siloxane sublayers can suppress these fluctuations, these sublayers remove the entropic penalty for the FE structure and make the FE structure more favorable.^{12c} If the oligosiloxane sublayers are disturbed (short spacers, long alkyl chains, or small siloxane units), the entropic effect becomes more important, which is favorable for the AF organization. However, in addition to this entropic effect, there should also be an energetic stabilization of a synpolar FE structure by these sublayers. The reasons for this energetic effect are not completely clear, and further investigations are required.

In addition, with increasing length of the alkyl chains, steric effects also become important, and this leads to a transition from smectic phases via undulated smectic phases to an oblique columnar phase formed by ribbon-like layer fragments. Simultaneously, the switching process changes from a rotation around a cone in the smectic phases, which retains the layer chirality, to a switching around the long axis in the columnar phases, which reverses the layer chirality.

In summary, this work has contributed to a significantly improved understanding of the relations between molecular structure, emergence of polar order, and supramolecular chirality in bent-core systems. It highlights the importance of the engineering of interfaces for directed LC materials design.⁵⁹

Acknowledgment. The work was supported by the DFG (GRK 894/1) and the Fonds der Chemischen Industrie; R.A.R. is grateful to the Alexander von Humboldt Foundation for the research fellowship. We thank Noel Clark (University of Colorado at Boulder) for helpful discussions.

Note Added after ASAP Publication: In the version published on the Internet February 9, 2006, the central biphenyl benzoate units were drawn in the wrong direction in the formula of compounds **En-9B12** and **Si_x-mBn** in Scheme 1 and in Tables 1–3. The formula are correct in the version published February 22, 2006, and in the print version.

- (58) Related transitions between AF and FE switching were observed for B₅ phases, where the FE switching phase appears at low temperature: (a) Nadasi, H.; Weissflog, W.; Eremin, A.; Pelzl, G.; Diele, S.; Das, B.; Grande, S. *J. Mater. Chem.* **2002**, *12*, 1316–1324. It was also observed in mixtures of FE and AF switching materials with B₂-type phases, but in this case, the phase sequence is reversed, here the FE switching phase is the high-temperature phase: (b) Kumazawa, K.; Nakata, M.; Araoka, F.; Takanishi, Y.; Ishikawa, K.; Watanabe, J.; Takezoe, H. *J. Mater. Chem.* **2004**, *14*, 157–164.
- (59) In a similar way, bulky hydrocarbon units were recently used to influence the interlayer correlation in SmC phases of rod-like molecules: Cowling, S. J.; Hall, A. W.; Goodby, J. W. *Liq. Cryst.* **2005**, *32*, 1483–1498.

Supporting Information Available: Figures explaining the occurrence of suprastructural chirality (S1) and possible organizations in the distinct Col_{ob}P_A phases (S6); switching current response curves for compounds **12B12** (S3) and **Si₃-11B16** (S11); textures of the SmCP_A phase (S2), the Col_r phase (S4), the SmC_sP_F^[*/○] phase of **Si₃-6B12** (S8), the Col_{ob}P_A phase of **Si₃-11B20** (S5); optical changes during the switching of **Si₁-11B12** (S12); diffraction pattern of **Si₃-11B20**, **Si₃-6B12**, and

Si₃-9B12 (S7, S9, and S10), X-ray data (Table S1); transition temperatures of the olefinic precursors **En-(*m*-2)Bn** (Tables S2, S3), experimental procedures and analytical data (NMR, MS, elemental analysis) of the reported compounds. This material is available free of charge via the Internet at <http://pubs.acs.org>.

JA057685T